

N71-30263

NASA TECHNICAL TRANSLATION

NASA TT F-13,727

SURVEY OF THE EXPERIMENTAL CAPABILITIES OF THE  
O.N.E.R.A. HYDRODYNAMIC TUNNEL,  
WHICH OFFERS FLOW VISUALIZATION

H. Werle

Translation of "Aperçu sur les Possibilités  
Experimentales du Tunnel Hydrodynamique a  
Visualisation de L'O.N.E.R.A.", National  
Office National D'Etudes et de Recherches Aero-  
nautiques, ONERA Note Technique No. 48,  
1958, 36 pages

CASE FILE  
COPY

NATIONAL AERONAUTICS AND SPACE ADMINISTRATION  
WASHINGTON, D. C. 20546

JULY 1971

## TABLE OF CONTENTS

	<u>Page</u>
ABSTRACT .....	1
1. <u>Introduction</u> .....	1
2. <u>Experimental Techniques</u> .....	2
2.1. — The tunnel .....	2
2.2. — Models .....	3
2.3. — Visualization Methods .....	3
2.3.1. — Injection of colored liquid .....	3
2.3.2. — Use of air bubbles .....	5
2.4. — The apparatus .....	7
3. <u>Some Examples of Aerodynamic Studies</u> .....	8
3.1. — Example No. 1: "Study of stream defectors" .....	8
3.2. — Example No. 2: "Laminar boundary layer and turbulent boundary layer" .....	10
3.3. — Example No. 3: "Study of planar flows" .....	11
3.4. — Example No. 4: "Study of parietal flows" .....	12
3.5. — Example No. 5: "Study of vortices" .....	16
3.6. — Example No. 6: "Interaction between external and internal flows" .....	17
3.7. — Example No. 7: "Study of separation near the leading edge" .....	17
3.8. — Example No. 8: "Hyperlifting by a deflected engine jet" .....	19
3.9. — Example No. 9: "Transient studies" .....	20
4. <u>Conclusion</u> .....	21
REFERENCES .....	22
Figures 1-74 .....	26

SURVEY OF THE EXPERIMENTAL CAPABILITIES OF THE  
O.N.E.R.A. HYDRODYNAMIC TUNNEL,  
WHICH OFFERS FLOW VISUALIZATION

H. Werle

ABSTRACT. Various publications have already described the O.N.E.R.A. hydrodynamic tunnel<sup>(1)</sup> for the visualization of low-velocity flow ( $R \sim 10^4$ ) and some of its applications to theoretical and experimental aerodynamics [2] and [3].

/1\*

After a review of the conditions in which this "water wind-tunnel" is used, this report discusses its present experimental capabilities and describes several examples of recent research.

1. Introduction

Although it is difficult, if not impossible, to have complete correspondence between hydrodynamic and incompressible aerodynamic flows, experience shows that tests in low-velocity water ( $R \sim 10^4$ ) can, in many cases, provide very instructive "pictures" of the aerodynamic field, and useful information about complex phenomena which are difficult to reveal in air. Experience shows that the system has achieved one of the design goals of Maurice Roy, Director of O.N.E.R.A. in projecting and building this extremely economical tunnel at Chatillon.

---

\* Numbers in the margin indicate pagination in the original foreign text.

(1) During the study, the classic techniques in this area, chiefly the works of Marey, Nogues, Toussaint, Carafoli, Favre, Valensi, Chartier, Bourot, Sackmann, and others [1] have been used extensively.

In particular, it has been confirmed that experimentation in water, often more precise and more delicate, and here much less costly than in air, represents for many cases one of the best methods of study, particularly for certain basic research. Of course, the hydrodynamic tunnel cannot replace all other experimental techniques; it can nearly always complement them.

The O.N.E.R.A. tunnel is characterized by the great simplicity of the apparatus and operating procedures. It provides the tests which are basic to all valid experimentation:

- tests of the device accuracy by obligatory repetitions of the runs;
- tests of the validity of the visualization methods with the aid of constant cross-checks among the different procedures.

By means of these precautions, it is possible to carry out systematic tests which, for each study, reveal the flow mechanism and the influence of the principal parameters.

These precise results can lead to valuable comparisons with theory, or with experimental results obtained in another way under conditions similar to those of the tunnel: incompressible fluid, laminar flow, etc.

They are only qualitative indications when these conditions are clearly different. In this case, their correct interpretation and their transfer to aerodynamics become tricky.

## 2. Experimental Techniques

/2

### 2.1. — The tunnel (Figure 1) —

The tunnel, built according to the design of M. Maurice Roy, is a vertical open loop.

It runs in "spurts" under the action of gravity, with the inevitable requirements of this type of device: refilling, settling, limited test duration, variable pressure, etc.

There are a certain number of interchangeable test sections, whose geometric and hydraulic characteristics are listed in the following table.

## 2.2. — Models (Figures 5 and 6) —

The different model types and their mounting in the test section of the tunnel are analogous to those used in wind tunnels.

Their respective advantages and disadvantages have been described several times [3].

The models are generally made of brass or plexiglass, or else cast in plastic [4]. Their internal structure, which is more or less complicated, contains the channels necessary for injecting colored liquid, or for removal or addition of fluid for tests with aspiration or venting.

## 2.3. — Visualization Methods —

The different techniques for visualizing hydraulic flows are quite numerous [5], and some have been tested at the O.N.E.R.A. tunnel [6] and [7].

Only the two procedures which have been used for most of the experiments /3 will be mentioned here:

### 2.3.1. — Injection of colored liquid [8] —

This procedure has been perfected in certain respects to satisfy conditions imposed by different problems — in particular, by boundary-layer studies [9] to [11].

Figure	Type of test section	Cross-section (cm x cm)	Normal velocity (cm/s)	Duration of test at normal velocity (min)	Maximum velocity (cm/s)	Normal use	Example of test
1	Normal, guided	22 x 22	10	2	15	Laminar flow 2D & 3D	Examples 4 thru 9
2	Free 1 part guided	10 x 22	22	2	33	Free-stream 2D	Example 1
	With 1 part free	15.6 x 22					
3	Reduced, guided	10 x 10	10 to 50	2 to 10	70	Turbulent flow 2D & 3D	Example 2
4	Flat, guided	1 x 16	10 to 50	12 to 60	60	Flow in 2D	Example 3

Colored liquid: The mixture used is prepared from:

- homogenized milk (giving the necessary opacity for photos),
- alcohol (to restore the exact density of the water),
- dye (to facilitate individualization of the different colored streamlets), and especially water (which almost completely eliminates the viscosity difference).

In some cases, use of a red dye which rapidly turns green on dilution helps reveal zones of separation, zones of jet mixing with external flow, and even regions of transition from laminar to turbulent flow (Figure 70).

Injectors: Different types of injectors and modes of injection have been used; their advantages, disadvantages, and applications are given in the following table.

Modulation of injected flow: The dotting of the stream lines obtained this way allows: /4

- simple marking of each element of the milky streamlet [12],
- evaluation of velocities along the different streamlets (Figure 23).

In the case of injection of a small flow at a wall, this modulation gives rise to waves which are displaced downstream, and are progressively deformed under the influence of velocity differences in the flow. In this way, the velocity profile can be determined (Figure 61) [13].

#### 2.3.2. — Use of air bubbles [14] and [15] —

By this technique, one can obtain a very high density distribution of bubbles within the fluid with remarkable homogeneity (diameter from 1/20 to 1/10 mm). All that is required is addition of an emulsifier to the water during filling.

Type of injector	Advantages	Disadvantages	Main uses (steady-state regime)	Other uses
Holes on model surface	<ul style="list-style-type: none"> <li>- no wake</li> <li>- control is easy and independent of flow from each hole</li> </ul>	<ul style="list-style-type: none"> <li>- limited visualization near wing</li> <li>- beginning of a streamlet from the hole is not a streamline (jet effect)</li> <li>- difficult; limited number of holes</li> </ul>	visualization of streamlines of: <ul style="list-style-type: none"> <li>- exterior flow (high-rate)</li> <li>- flow within the boundary layer (low-rate)</li> <li>- parietal flow (quasi-zero flow)</li> </ul> See Figures 64 and 65.	Showing regions of separation, of "dead" water, of wake by injection for short periods into these regions. Coloring of jets (venting)  See Figures 12 and 18.  This can be superposed on the bubble method.
Ramp of holes	<ul style="list-style-type: none"> <li>- extended visualization of the whole aerodynamic field</li> </ul>	<ul style="list-style-type: none"> <li>- wake of the ramp</li> <li>- delicate adjustments</li> <li>- necessity of placing the ramp in the converger</li> <li>- necessity of a converger with a high contraction ratio</li> </ul>	behavior of streamlines in the entire aerodynamic field  See Figures 17 to 23	See Figures 38 and 48.  Revealing regions of turbulence (mixing of colored liquids, dilution of colored liquid).  See Figures 66, 70 and 73.
Single-emission probe	visualization upstream of the model with minimum perturbation	<ul style="list-style-type: none"> <li>- visualization limited to a small part of the field</li> <li>- delicate adjustments</li> </ul>	visualization of a stream line or of an isolated current sheet (depending on the model of the probe)	

The air bubbles show the flow in thin transverse or longitudinal cross-sections of the test section (see Figures 33 and 8, respectively). Depending on the exposure time, photographs record the trajectories (Figure 44) or small elements of the trajectories of the bubbles (Figure 45) projected on the plane visualized.

For steady-state laminar flow, these trajectories correctly represent stream lines except in regions of very high normal acceleration.

Zones of very low velocity generally end up empty of bubbles. This is the case for the boundary layer in contact with the surface of a model when the flow is laminar (see Figure 15).

Any turbulence is shown by the disappearance of this bubble-free layer and the presence of trajectories which intersect (see Figure 16).

For steady-state laminar flow, the small elements of the trajectories reveal the behavior of the velocity field, and in certain cases allow lines of constant velocity to be traced.

#### 2.4. — The apparatus —

The entire apparatus is now being used for adjustment and measurement of the parameters (see Figures 1 to 6), for recording (visual, photographic, and cinematographic), and for analysis of tests (projectors).

We shall merely mention use of certain devices during tests to produce slow and continuous variations of certain parameters (incidence of a model, setting of a flap, position of a jet engine, velocity and direction of a jet, etc.).

Systematic use of cinematographic recording (16 mm) makes possible:

- 1) production of short films, easy to distribute, which summarize long series of tests,
- 2) convenient study of certain phenomena
  - by repeated projection,
  - by the large scale of the projections (views of details),
  - by slow-motion (for rapid flows)
  - or by accelerated projection (to show the continuous variation of a parameter which must be slow during the test to conserve quasi-steady-state flow),
- 3) comparison, via composite views, of several flows corresponding to test conditions which are identical except for one parameter: /5

for example,

juxtaposed views of top and bottom surfaces, of exterior flow and parietal flow, of flow around models of different shapes,

or else,

superposed views of flow with and without venting [in this case, each flow is visualized with a differently-colored liquid (see Figures 73 and 74)].

### 3. Some Examples of Aerodynamic Studies<sup>(2)</sup>

#### 3.1. — Example No. 1: "Study of stream deflectors" —

(Example of tests carried out in the free section)

---

<sup>(2)</sup> It is important to note the considerable contribution of the late M. Maxime Degorce, Technician, to the tests carried out during these latter years.

A uniform free stream, for example, that which emerges into the free part of a test section, can be deviated by mechanical or pneumatic means.

Different types of deflectors based on these principles have been tested in the tunnel. In each case, it has been possible to determine the mechanism of deflection and the effectiveness of the device studied.

One method (Figure 7) consists of a grill of four superposed thin vanes, placed at the exit of the guided portion of the test section. The setting of the vanes produces a stream deflection downstream of the device. The deflected flow obtained is relatively good, though it is marred by the presence of a wake from the vanes, and vortices appear at the edges of the stream (Figure 8).

A second mechanical device is made up of a set of spoilers placed normal to the wall in the guided part of the test section, near the step. This set is controlled by an orientable arm which permits adjustment of the angle between the direction of the upstream flow and the line connecting the upper edges of the spoilers (see Figures 9 and 10).

The flow over this device is characterized by separation from the wall upstream of the first spoiler, and a stable vortex just ahead of each of the spoilers.

Although the asymmetric position of the system in the test section eliminates parasitic wakes, it does, however, cause a certain nonuniformity of flow, and its usefulness is limited to small deflection angles.

Use of venting jets more or less normal to the wall of the test section is the basis of the so-called pneumatic deflection devices.

The fluid flap issuing from a venting slit just upstream of the step produces a deviation and contraction of the main stream, which are functions

of the angle the jet makes with the direction of the upstream current and of the momentum-flow coefficient of the jet.

The flow mechanism near the jet is characterized (Figures 11 and 13):

16

- on the one hand, by the presence of a region of detachment from the wall upstream of the venting slit, which contains a stable vortex,
- on the other hand, by inductive effects of the jet over the whole length of the fluid flap, which curves progressively inward under the effect of the general current.

In the case of venting normal to the wall, the deflection and contraction obtained increase with the momentum-flow coefficient of the jet. The deflection obtained can become large (Figure 14).

A device with two symmetric jets is used to obtain contraction without producing deflection (Figure 12).

The results of these tests are in good agreement with those given by G. Ernst [16].

Comparison among the different deflectors makes evident the clear superiority of the pneumatic techniques over the mechanical ones when a large deflection is needed, with good uniformity of the deflected stream.

3.2. — Example No. 2: "Laminar boundary layer and turbulent boundary layer" —  
(Example of tests carried out in the reduced guided section)

The relatively extensive range of flow velocities obtained in the guided test-section with reduced cross-section makes it particularly suitable for studies involving turbulence.

The example given here concerns the boundary layer of a plane plate at zero incidence in a uniform steady-state stream.

The plate used has a relative thickness of 10%, and is rounded at the leading edge and beveled at the trailing edge.

At low velocity (Figure 15), laminarity of the boundary layer is confirmed by the presence of the bubble-free layer in contact with the wing surface, and by the highly parallel stream lines; it extends to a point near the trailing edge. The laminar structure of the separation at the beginning of the after bevel (return stream along the bevel, stream in the sense of the general flow near the separation surface) can be seen clearly.

When the velocity is high (see Figure 16), the laminar boundary layer separates near the leading edge normal to the discontinuity in curvature of the profile, the transition is triggered, and is followed by the turbulent re-attachment described by Melwil Jones [17]. Aft of this bulb a turbulent boundary layer develops whose velocity fluctuations are recorded in photos as disordered bubble trajectories.

Finally, the turbulent separation which ends up on the beveled portion of the trailing edge produces less wake than the preceding case.

### 3.3. — Example No. 3: "Study of planar flows" —

(Example of studies in the flat test section)

The flat section designed for the study of planar flows is similar in certain respects to the hydraulic cells developed and used by E. Carafoli and A. Toussaint [8], by A. Favre [18], and by L. Sackmann [19].

Because of its extensive range of flow velocities, this device makes it 17 possible to study different flow regimes around an obstacle as a function of the Reynolds number: see Figures 17 and 18.

Comparison between flow at the center of the test section (Figure 19) and flow at the wall (Figure 20) shows that only the former can be considered planar. The region empty of a colored liquid, which appears near the leading edge of the profile, is the place where rolling motion was observed by L. Sackmann on a wall near obstacles [19].

Another example of such research is that on venting at the trailing edge of a truncated profile at zero incidence. Figures 21, 22, and 23 show the inductive effects of a jet which "aspirates" the colored streamlets, as well as the influence of jet orientation on the position of the stagnation point.

The validity of these results is corroborated by remarkable visualizations in air, using smoke, by C. D. Perkins, D. C. Hazen, and R. F. Lehnert [20] and [21], and, more recently, by A. M. Lippisch [22].

#### 3.4. — Example No. 4: "Study of parietal flows" —

(This example and those which follow concern tests in the normal test section)

After the development of the colored-emission technique, it was possible to take up studies of relatively thin boundary layers, at the initiative and under the direction of R. Legendre.

In the case of steady-state laminar flow, the parietal stream lines of an obstacle could be revealed, that is, the limiting positions of the stream lines as they tend toward the wall of this obstacle.

The first example is the study of an elongated ellipsoid of revolution inclined to the flow (Figure 62).

Certain difficulties in the interpretation of the phenomena observed at  $10^\circ$  incidence near the symmetry plane at the beginning of separation on the upper face have contributed to a revision of customary ideas about separation, which are too closely connected to its well-known image in planar flow [10].

This necessity of giving a general definition of three-dimensional separation has led to different theoretical studies<sup>(3)</sup> [23] and [24], whose description is beyond the scope of this report, and to certain tests which have confirmed the existence of different singularities and characteristic elements in parietal flow.

These elements, described by R. Legendre [24], and clearly visible in Figures 24 to 31, are the following:

- point of isotropic convergence (umbilicus) at the center of the upstream face of a disk translated normal to its plane (Figure 24).
- point of convergence in the case of asymmetric separation on the bottom of a flattened ellipsoid at  $2.5^\circ$  incidence (Figure 25).
- line of separation on the upper surface of a swept wing with nonzero incidence, "quasi-enveloped" in parietal stream lines upstream (injection at the leading edge) and downstream (injection within the separated region): see Figure 26.
- parting line on the bottom face of a swept wing with nonzero incidence, /8  
between the part of the flow which bends along the leading edge on the upper surface, and that which rejoins the trailing edge directly (Figure 27).
- partition point located at the intersection of the separation line with the median plane on the top face of a flattened ellipsoid of revolution with nonzero incidence (Figure 28).
- inward curve (very accentuated) of the parietal stream lines toward the marginal fluid flap which exits normal to the chord plane on the

---

(3) Notably that of E. Eichelbrenner.

bottom face of a rectangular wing of limited span, at zero incidence (Figure 29).

The photo also shows the outlining of the marginal edge by one part of the upper parietal stream lines.

The study of marginal, or even peripheral, venting (Figure 74) [25], belongs to the systematic tests in the tunnel to define the influence of venting on the flow around wings of different shapes and for different positions of the slits (Figures 71 and 72) [26].

— point of spiral convergence observed, for example, on the top face of a delta wing with nonzero incidence (near the trailing edge and at about midspan on each half-wing for incidence of  $8^\circ$ ): Figure 30.

Examination of the photo also shows the divergence of the parietal stream lines in the central portion of the top face of this thick wing with rounded leading edge, as well as the presence of a separated region near each of the two after points.

This study of parietal flow has been extended to the case of a thin delta wing with pointed leading edge (Figures 64 and 65).

The experiment has cast light on the flow scheme proposed by Maurice Roy [27] and [28], in particular, the sheet rolled into a "cone" detached along the leading edge (Figure 64).

The structure of this flow is seen again in the parietal flow over the upper surface (Figure 65), where one can distinguish:

- the quiet part of the flow, located in the middle (in red),
- the region swept by vortices (in yellow at midchord),

- the region under the "cone", near the leading edge, where the flow "returns" toward the leading edge, where separation is produced (in blue).

Absence of turbulent character in the flow over the bottom surface (Figure 67) contrasts with the vortices on the upper surface (Figure 66) which issue from the upstream point, and are particularly well organized at higher incidences ( $i = 12^\circ$ ).

A recent study has been able to outline the nearly conical structure of such a flow [12].

All these observations in water [3] confirm the results of visualizations made in air [29] and [30].

The mechanism of flow around a vortex generator contains a number of the characteristic elements analyzed above (Figure 31).

The generator mentioned in the example consists of a small rectangular blade with small span, arranged normal to the upper wall upstream of a rectangular wing, and placed at an angle to the current. /9

The parietal injections reveal:

- (1) the partition point and the region empty of colored liquid upstream of the leading edge,
- (2) the point of spiral convergence near the trailing edge on the upper face, the point of departure of a vortex which follows this trailing edge before it joins the marginal vortex of the wing.

### 3.5. — Example No. 5: "Study of vortices" —

Among the principal types of vortices whose study has been undertaken at the O.N.E.R.A. tunnel, we should mention:

- vortices at the apex of highly swept wings, as discussed in the preceding paragraph (see also [31]),
- marginal vortices of rectangular wings of limited span, which result either from venting (Figures 71 and 72) [26], or from incidence (Figure 60) — the classic case which has been the subject of numerous publications [32] to [35].
- vortices on the upper surface of slender bodies inclined to the current (Figures 62 and 63).

The vortices observed on a model of this type — for example, on a cylinder tipped by an ogive without a point — appear at about  $8^\circ$ , are displaced progressively as a function of the incidence of the model (Figure 34), and are particularly well developed at high incidence, for example, at  $i = 20^\circ$  (Figures 32 and 33).

Figure 33, which represents a transverse cross-section of the flow, shows the existence of a partition point of the transverse quasi-flow above the two vortices and in the symmetry plane.

Studies of a fuselage alone have been followed by those of various engine models, for example, a fuselage with a wing mounted in canard configuration with or without empennage, to investigate the interaction of fuselage with forward and after wings.

Figure 35 gives the example of a forward rectangular wing of very short span, whose incidence  $\alpha$  is  $10^\circ$ , and of a slightly inclined fuselage ( $i = 5^\circ$ ).

The marginal vortices of the forward wing are definitely influenced by the presence of the cylinder; examination of their trajectories in the projection onto the transverse plane (Figure 36) shows that the behavior of the curves, the direction of displacement, or even the equilibrium (trajectory reduced to a point) in the transverse plane depend closely on the configuration parameters.

These results qualitatively confirm the theory studied by von Baranoff [36].

The presence of an after wing further complicates the flow, particularly at high incidences, where there is a superposition of the effects of vortices produced by the fuselage and by the forward and after wings (Figure 68).

### 3.6. — Example No. 6: "Interaction between external and internal flows" —

The effect of a jet leaving the rear of a model along the longitudinal axis in planar flow, has already been mentioned in paragraph 3.3 (Figure 21).

In the case of an elongated ellipsoid of revolution inclined slightly to /10 the current, the effect of such a jet is extremely clear: the jet literally aspires the flow and makes every trace of separation disappear (compare Figures 37 and 38 with Figures 39 and 40), even in parietal flow (Figure 41).

A rather favorable effect of internal flow on external flow underlines the importance of the problem — for example, in the case of the exhaust of a jet engine (Figure 69) [37].

### 3.7. — Example No. 7: "Study of separation near the leading edge" —

The contribution of the hydrodynamic tunnel to the immense problem of separation — in particular, to the experimental study of the conditions for separation near a leading edge — is limited to revealing the flow mechanism.

Due to visualization by air bubbles, it is possible to determine in each case:

- the behavior of the stream lines and the positions of the stagnation, separation, and transition points (see Figure 44),
- the behavior of the velocity field (see Figure 45) and from this, the behavior of the lines of constant velocity,
- the extent and character of the separation, as well as whether re-attachment occurs (see Figure 46),
- finally, the efficiency of different methods of handling separation, notably that of tangential venting with or without adjustment of the profile (breaking the leading edge), which suppresses separation completely (see Figure 47).

This type of tangential-venting device easily allows hyperlifting of a wing/ventilated trailing-edge flap combination (see Figure 70) [42].

This experimental study confirms the existence of different types of separation, described by D. Kuchemann [38], among others:

- flow without leading-edge separation (Figure 42): this is the case for low incidence, with separation appearing only beyond midchord, as has been determined during a previous study [13];
- flow with generalized detachment (Figure 43): this is the case at high incidence. Separation begins at the leading edge and has a rather reduced laminar part, followed by a turbulent region which prolongs the wake of the wing;
- flow with a separation bulb (Figure 44): this separation characterizes flow with high circulation, obtained, for example, by trailing-edge venting (Figure 46). This latter photo shows the inductive effects of the jet leaving normal to the chord, principally the presence of turbulent re-attachment near midchord.

Finally, the tests have made apparent in each case the influence of the principal parameters: incidence of the profile, coefficient of momentum flow of the different venting jets, etc.

### 3.8. — Example No. 8: "Hyperlifting by a deflected engine jet" —

Hyperlifting of a wing can be obtained, as mentioned in the preceding paragraph, by the action of a fluid flap leaving a venting slit at the trailing edge nearly normal to the plane of the model.

The possible application of this very pure method to real aircraft would, /11 however, lead to a considerable complication of the interior structure of the airfoils.

A form which seems better adapted to aircraft architecture, and which has been the object of several tests, especially by N.A.C.A. [39], consists of diverting the jet of an under-wing engine toward the trailing-edge flap. The flap contains a slit which enables the jet to pass over the upper face, from which it leaves tangentially (Figure 50).

The work presented in this report only concerns flow in the symmetry plane of the engine-model ensemble, the rectangular wing being fixed between the walls, and the likeness of the engine mounted on an articulated strut (Figure 6).

The deflection of the engine jet is obtained by mechanical means (flap, Figures 48 and 49) or pneumatic devices (auxiliary jet, Figures 50 and 51), whose efficiency is comparable to the different types of deflectors studied previously (Example No. 1).

The increase in circulation thus obtained (see Figures 48 to 51) is expressed, in particular, by displacement of the stagnation point and disappearance of the separation regions observed in the absence of the jet (Figure 73).

Study of the influence of different configurational and flow parameters has thus allowed us to define the following for the average test conditions:

- the minimum jet necessary,
- the maximum possible position of the bending flap,
- the optimum region for installing the engine,
- the optimum control of the setting of the deflector flap or jet deflector (the latter method is clearly superior to the former), etc.

### 3.9. — Example No. 9: "Transient studies" —

Without insisting on the difficulties of visualization and correct interpretation of tests made outside the steady-state region, some examples of this type of research should, however, be mentioned. They fall into two categories:

— periodic motions: wing or flap driven by flapping or oscillation, intermittent venting jet, etc., such as planar nonsteady movements with constant circulation [40].

— starting motions:

Example: disk in translation normal to its plane:

Tests reveal formation of a toroidal vortex during starting (Figures 52 and 53) [41]. This vortex becomes disorganized, and is replaced by a region of dead fluid with a turbulent boundary when the steady-state regime is established (Figure 54).

Example: sharp leading edge with nonzero incidence:

During starting, only a small part of the upper surface near the end of the leading edge is the site of separation, which appears as a vortex cylinder (Figure 55).

This bulb of separation is transformed into generalized separation when the flow becomes steady-state (Figure 56).

Example: thick profile at zero incidence:

The different phases of the test are characterized by:

- absence of separation and progressive thickening of the boundary layer (Figure 57) during the first part of starting,
- appearance of laminar separation which moves progressively upstream, as well as the formation and development of two symmetric vortices on the trailing edge (Figure 58) [41] /12 during the second part of starting,
- boundary extension of the separated region, prolonged by a wake with alternating vortices (Figure 59), the final stage of the steady-state regime.

#### 4. Conclusion

These few examples suffice to show that the hydrodynamic tunnel, despite its limitations, can make a useful contribution to aerodynamic research.

Based essentially on visualization, it allows one immediately to grasp the mechanism or the broad outlines of the most complex phenomena, using only extremely simple and inexpensive methods.

The wind-tunnel theoretician and experimenter will often find guiding ideas there, which are necessary to arrive at a better comprehension of the phenomena without too many false starts.

In this respect, the hydrodynamic tunnel is one of the best methods for teaching fundamental ideas of fluid mechanics.

## REFERENCES

/13

1. Nogues, P. Experimental Studies of Marey on Movement in Air and in Water. Publ. Scient. Techn. Ministere de l'Air, No. 25.  
  
Valensi, J., A. Favre, C. Chartier, J. M. Bourot and L. Sackmann: see below.  
  
Toussaint, A. and E. Carafoli: see [8].
2. Roy, Maurice. Contribution of Aeronautical Research to Progress in Aviation. O.N.E.R.A. Publication No. 90, 1957.
3. Werle, H. The Hydrodynamic Tunnel for Visualization, and Its Application to Aerodynamics. Communication to the Association Technique Maritime et Aeronautique, 1957 meeting.
4. —. Some Experimental Results on Swept Wings at Low Velocities, Obtained in a Hydrodynamic Tunnel. O.N.E.R.A., La Recherche Aeronautique, No. 41, 1954.
5. Dixmier, G. and L. Lansac. Contribution to the Technique of Precision Molding of Inexpensive Models in Mixed Polyester. O.N.E.R.A. Technical Note No. 20, June, 1954.
6. Balint, E. Techniques for Visualization of Flows. S.D.I.T. translation of article in Aircraft Engineering, June, 1953.
7. Werle, H. Visualization in the Hydrodynamic Tunnel. O.N.E.R.A., La Recherche Aeronautique, No. 33, 1953.
8. Laz, J. Methods for Visualization in the Hydrodynamic Tunnel. La Nature, No. 3267, July, 1957.
9. Rebuffet, P. Experimental Aerodynamics. Libraire Beranger (§ 4921).
10. Oudart, A. and E. A. Eichelbrenner. Method of Calculating a Three-Dimensional Boundary Layer. Application to a Slender Body Inclined to the Flow. O.N.E.R.A. Publication No. 76, 1955.
11. Eichelbrenner, E. A. and A. Oudart. Laminar Three-Dimensional Separation. O.N.E.R.A., La Recherche Aeronautique, No. 47, 1955.

12. Eichelbrenner, E. A. and H. Werle. Laminar Three-Dimensional Separation: The Case of a Flattened Ellipsoid with Nonzero Incidence. O.N.E.R.A., brief report in La Recherche Aeronautique, No. 49, 1956.
13. Werle, H. Attempt to Verify the Conicity of Flow Around a Thin Delta Wing with Nonzero Incidence. O.N.E.R.A., brief report in La Recherche Aeronautique, No. 63, 1958.
14. Eichelbrenner, E. A. and H. Werle. Laminar Two-Dimensional Separation: Comparison of Theory and Experiment. O.N.E.R.A., La Recherche Aeronautique, No. 51, 1956. /14
15. Birkhoff and Cagwood. Use of Air Bubbles. Journal of Applied Physics, Vol. 20, July, 1949, p. 646.
16. Lambourne, C. and S. Pusey. Some Visual Observations of Flow Over a Sweptback Wing in a Water Tunnel, with Particular Reference to High Incidences. C. P. No. 192. Aeronautical Research Council Current Papers, 1955.
17. Ernst, G. Guidance of an Aircraft by Deflection of an Engine Jet. Communication to the A.T.M.A., 1957 Meeting.
18. Jones, M. Journal of the Royal Aeronautical Society, Vol. 38, 1934, p. 753.
19. Favre, A. Contribution to the Experimental Study of Hydrodynamic Two-Dimensional Motion. Publ. Scient. Techn. Ministere de l'Air No. 137, 1938.
20. Sackmann, L. Fluid Flow Near Singularities of Obstacles. Publ. Scient. Techn. Ministere de l'Air No. 92, 1936.
21. Perkins, C. D. and D. C. Hazen. Preprint of the Royal Aeronautical Society, September, 1953.
22. Hazen, D. C. and R. F. Lehnert. Smoke Flow Studies Conducted at Princeton University. Report 290.
23. Lippisch, A. M. Flow Visualization. Article in Aeronautical Engineering Review, Vol. 17, No. 2, February, 1958.
24. Eichelbrenner, E. A. Laminar Separation in Three Dimensions on a Finite Obstacle. O.N.E.R.A., Publication No. 89, 1957.
25. Legendre, R. Separation of Three-Dimensional Laminar Flow. O.N.E.R.A., La Recherche Aeronautique, No. 54, 1956.
26. Werle, H. Influence of Peripheral Venting on the Flow Around a Rectangular Wing and a Flattened Ellipse. O.N.E.R.A., brief note in La Recherche Aeronautique, No. 62, 1958.

27. Poisson-Quinton, P. Some Physical Aspects of Venting of Aircraft Wings. Article in "Techniques et Sciences Aeronautiques", Vol. IV, July-August, 1958.
28. Roy, Maurice. Character of Flow Around a Highly Swept Wing. C. R. Acad. 15 Sci., Vol. 234, 1952, p. 2501.
29. —. On the Theory of the Delta Wing. Apical Vortices and Sheets with Cones. O.N.E.R.A., La Recherche Aeronautique, No. 56, 1957.
30. —. Comments on Turbulent Flow Around Swept Wings. Z. angew. Math. Phys., Vol. IXb, No. 5/6, 1958, p. 554.
31. Gresser, A. J. Parietal Injection of Smoke in a Subsonic Wind Tunnel. O.N.E.R.A., brief note in La Recherche Aeronautique, No. 63, 1958.
32. Ornberg, Torsten. Report on the Flow Around Delta Wings. K T H Aero T.N. 38, 1954.
33. Legendre, R. Flow Near the Forward Point of a Highly Swept Wing at Moderate Incidences. O.N.E.R.A., La Recherche Aeronautique, Nos. 30 and 31, 1952 and 1953.
34. Valensi, J. Application of the Method of Smoke Trails to the Study of Aerodynamic Fields. Publ. Scient. Techn. Ministere de l'Air No. 128, 1938.
35. Chartier, C. Experimental Study of Wing Wakes. Publ. Scient. Techn. Ministere de l'Air No. 178, 1942.
36. Bourot, J. M. Chronophotography of Aerodynamic Fields. Publ. Scient. Techn. Ministere de l'Air No. 226, 1949.
37. Spreiter, J. R. and A. H. Sacks. The Journal of the Aeronautical Sciences, Vol. 18, No. 1, January 1951.
38. Von Baranoff. Theory of the Interaction of a Fuselage with Forward and Aft Wings. O.N.E.R.A., in press.
39. Carriere, P. Interaction of External and Internal Flows at the Exhaust of a Jet Engine at Transsonic and Supersonic Velocities. Communication to Journees Internationales de Sciences Aeronautiques. Published by O.N.E.R.A., Paris, May 27-29, 1957.
40. Kuchemann, D. "Types of Flow on Swept Wings" with Special Reference to Free Boundaries and Vortex Sheets. Journal of the Royal Aeronautical Society, November, 1953.
41. Lowry, J. G., J. M. Riebe and S. P. Campbell. The Jet Augmented Flap. I.A.S. Preprint No. 715, January, 1957.

42. Werle, H. Plane Nonsteady Motions with Constant Circulation. Comparison of Theoretical and Experimental Results. O.N.E.R.A., La Recherche Aeronautique, No. 26, 1952.
43. Eck, Bruno. Technische Stromungslehre (Technical Theory of Fluid Flow). Springer, 1957, pp. 45 and 239.
44. Carriere, P., E. Eichelbrenner and P. Poisson-Quinton. Theoretical and Experimental Contribution to Boundary-Layer Control by Venting. Communication to the 1st International Congress of Aeronautical Sciences, Madrid, 1958.

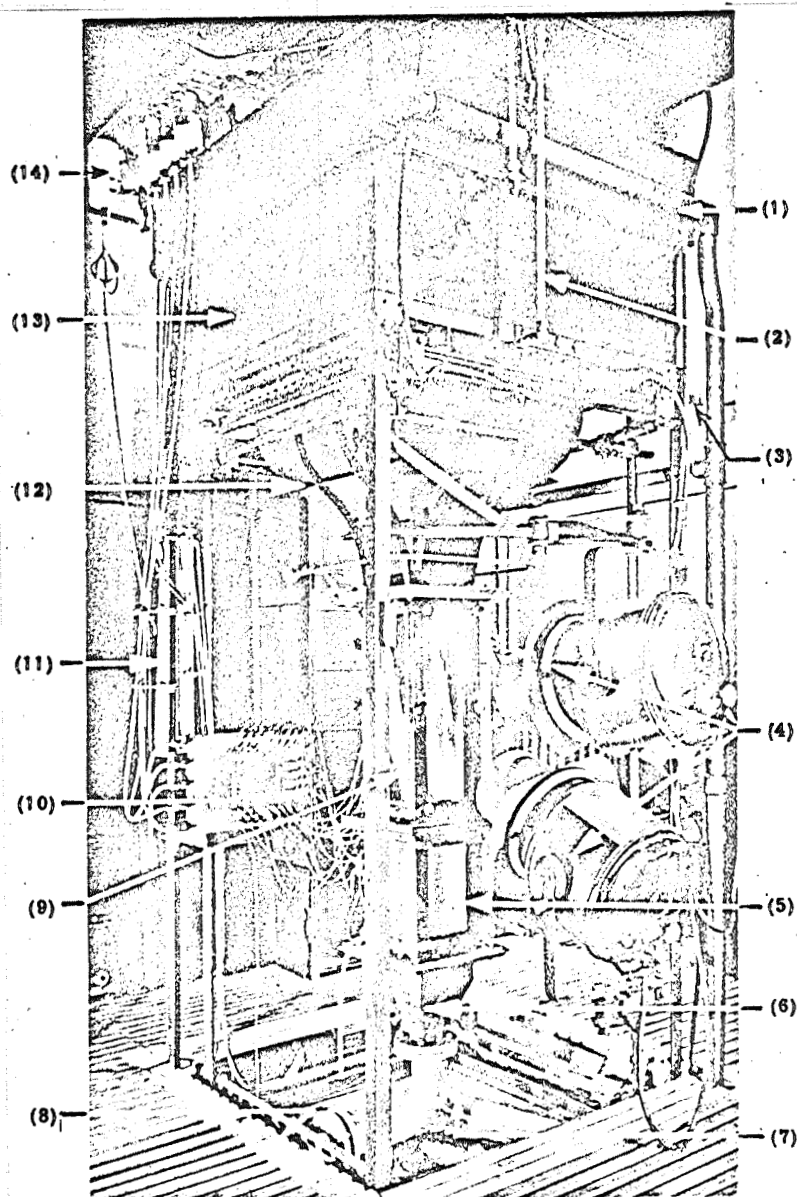


Figure 1. The hydrodynamic tunnel. 1 - overflow; 2 - level indicators; 3 - inlet pipe; 4 - projectors with adjustable diaphragms for illumination of cross-sections; 5 - extension of the test section; 6 - downstream converger; 7 - piping for venting and aspiration; 8 - to the main flow of the tunnel to measure the velocity of the flow; 9 - normal test section; 10 - control of colored injection; 11 - valve-flowmeter assembly for control and measurement of the fluid injected or removed; 12 - upstream converger (with honeycomb grid); 13 - reservoir for the tunnel; 14 - reservoir for colored fluid.

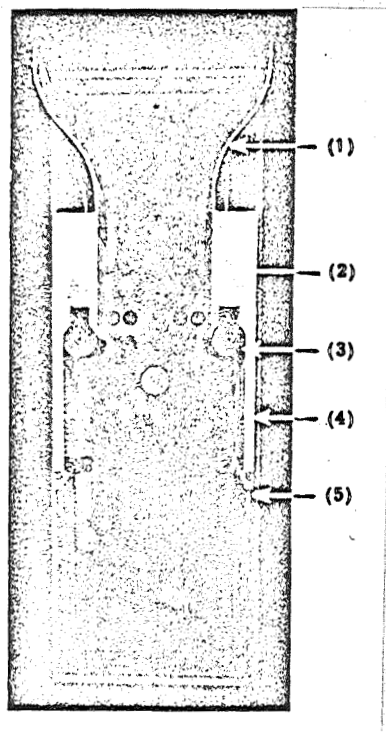


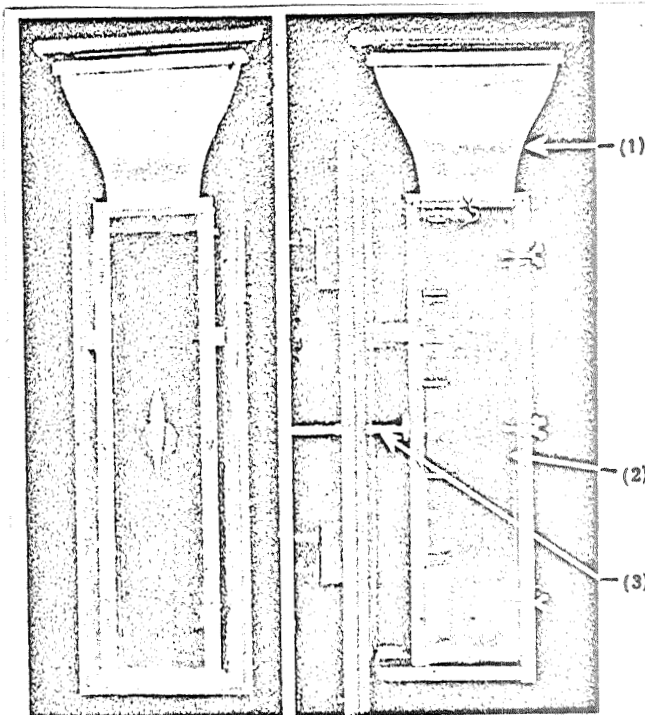
Figure 2. Free test section (within the normal section).

/17

1 - supplementary upstream converger;  
2 - guided part; 3 - orientable  
venting slits; 4 - free part; 5 -  
aspirating slits.

Figure 3. Reduced guided test section (within the normal section).

1 - supplementary upstream converger;  
2 - model mounted between the walls;  
3 - inlet for colored liquid and incidence control.



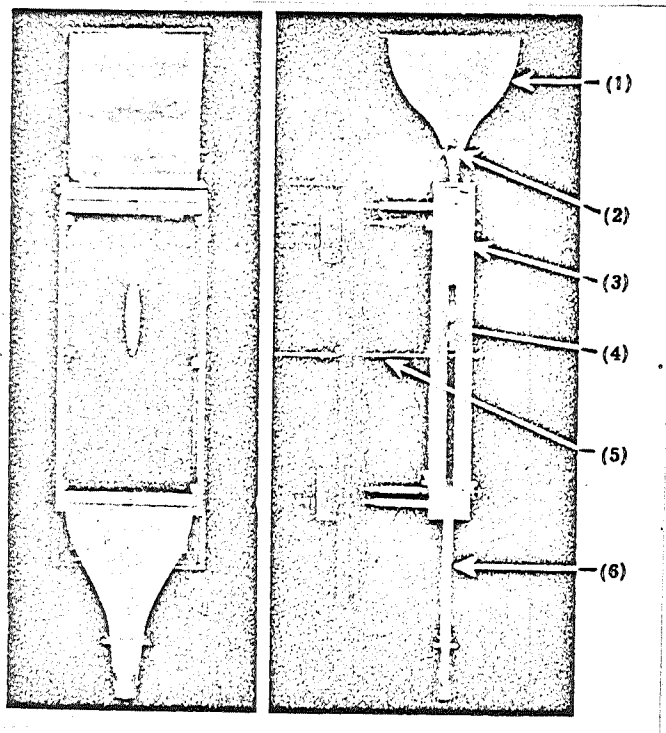
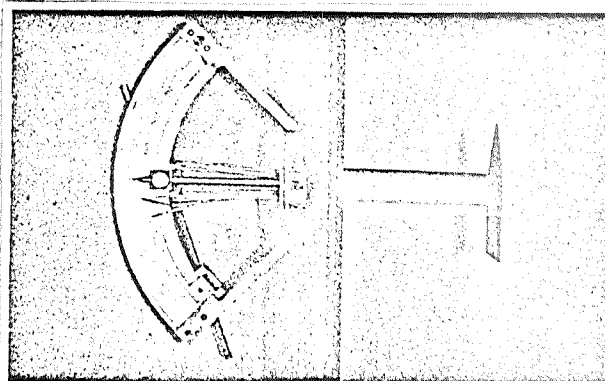


Figure 4. Flat guided test section (within the normal section).

1 - supplementary upstream converger; 2 - ramp of hole injectors for colored liquid at the center of the section; 3 - ramp of hole injectors at the section wall; 4 - model mounted between the walls; 5 - inlet for colored liquid or vented fluid and incidence control; 6 - supplementary downstream converger.

Figure 5. Entire delta wing mounted on an articulated strut.

Incidence of the wing can be varied slowly and continuously during the test without interrupting colored streamlets.



/18

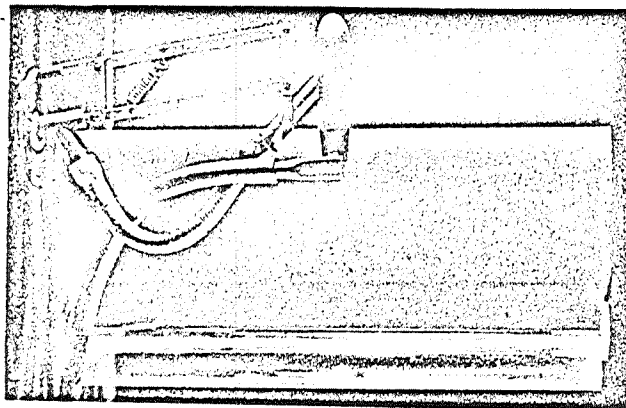


Figure 6. Rectangular wing fixed to the wall, with model jet engine mounted on articulated parallelogram. During test, the following can be varied:

- setting of the trailing-edge flap;
- position of the engine;
- jet velocity and its deflection toward the flap (obtained by an auxiliary jet).

} all without interrupting the flow of colored liquid.

Example No. 1 - "STUDY OF STREAM DEFLECTORS" - (Tests in the free section)

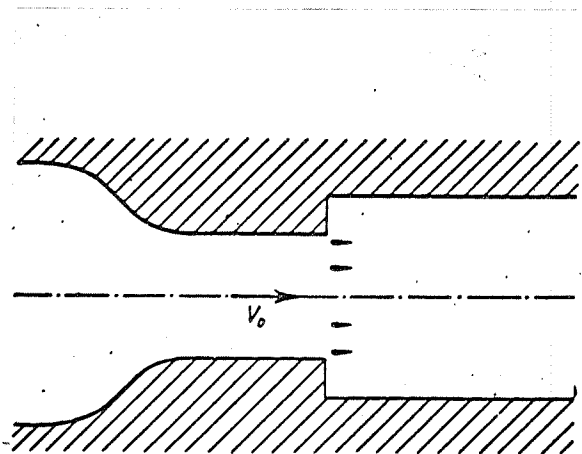


Figure 7. Diagram of the device with superposed vanes.

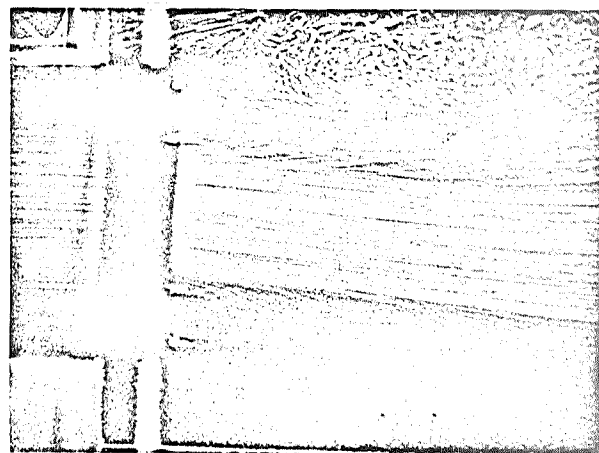


Figure 8. Flow deflected by a grill of vanes.

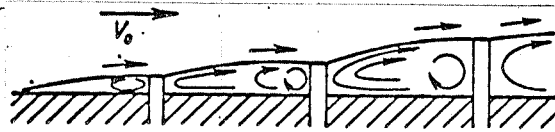


Figure 9. Diagram of the flow mechanism over spoilers.

/19

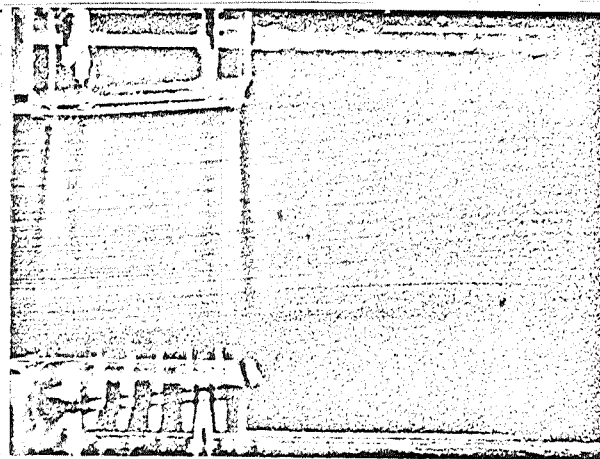


Figure 10. Flow deflected by a set of spoilers.

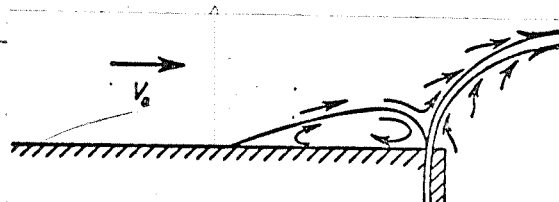


Figure 11. Diagram of the flow mechanism near a jet normal to the wall.



Figure 12. Contraction of the stream obtained by two symmetric normal jets.

Figure 13. Diagram of flow deflected by a jet.

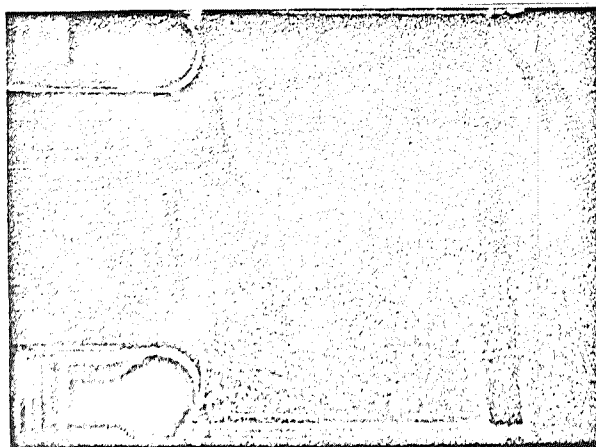
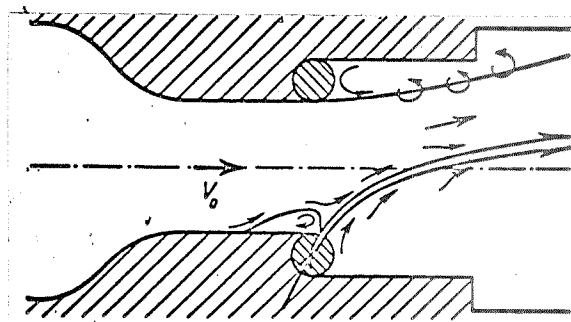
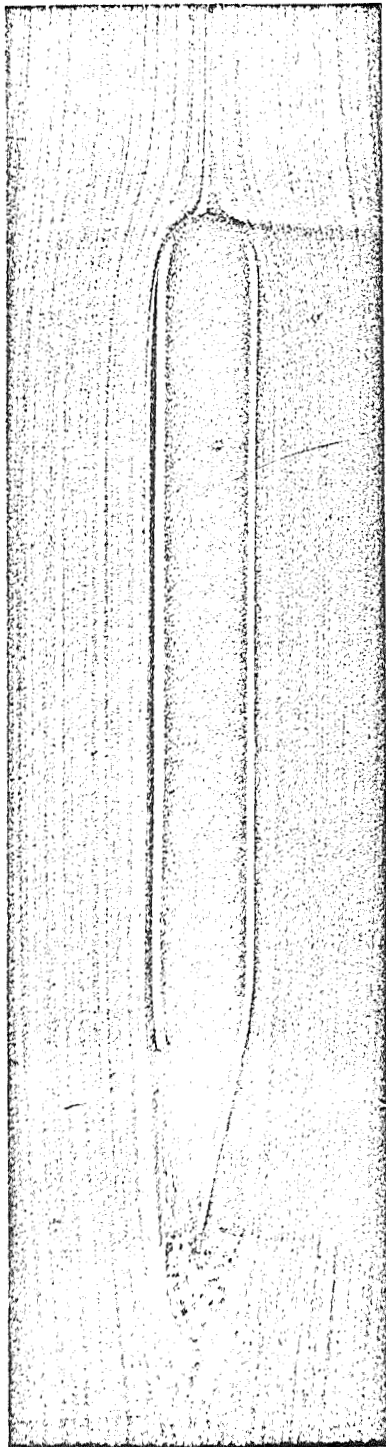


Figure 14. View of flow deflected by a jet.

Example No. 2 - "LAMINAR BOUNDARY LAYER AND TURBULENT BOUNDARY LAYER"  
(Tests in the reduced guided section)



/20

Figure 15. Low-velocity test.  
(Laminar boundary layer and laminar separation).

FLOW AROUND A PLATE MODEL WITH ZERO INCIDENCE

Example No. 2 - "LAMINAR BOUNDARY LAYER AND TURBULENT BOUNDARY LAYER"  
(Tests in the reduced guided section)

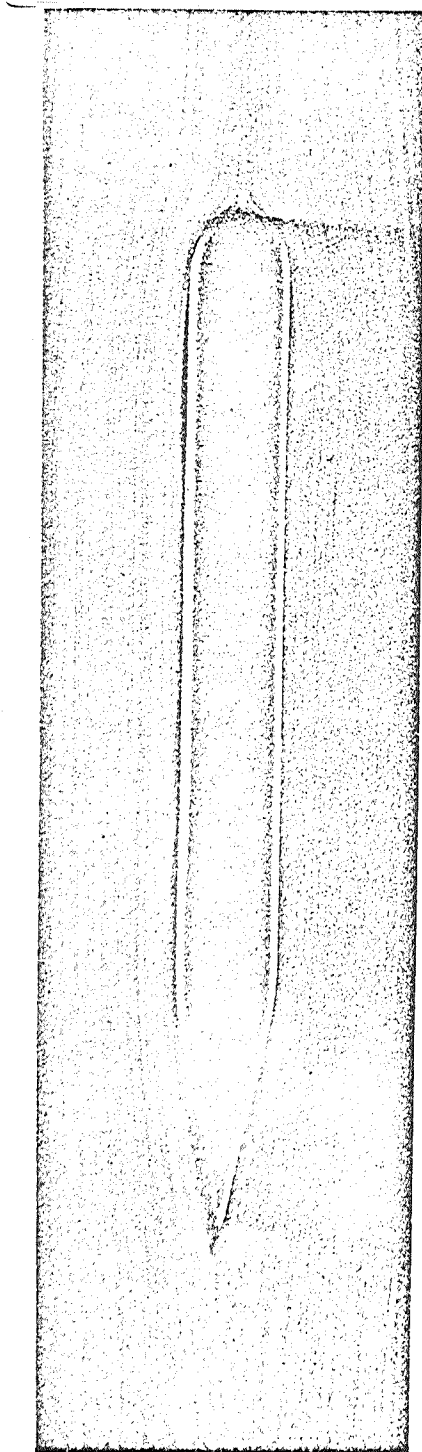


Figure 16. High-velocity test.  
(Bulb of separation near leading edge, with turbulent re-attachment followed by turbulent boundary layer and turbulent separation).

FLOW AROUND A PLATE MODEL WITH ZERO INCIDENCE

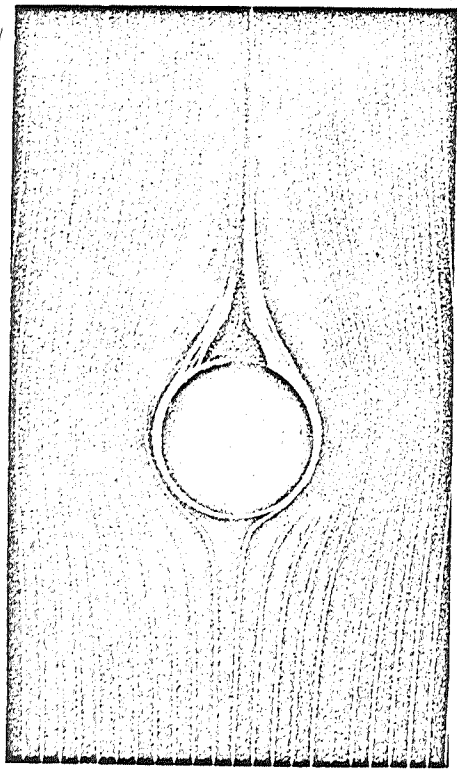


Figure 17. Low-velocity flow.

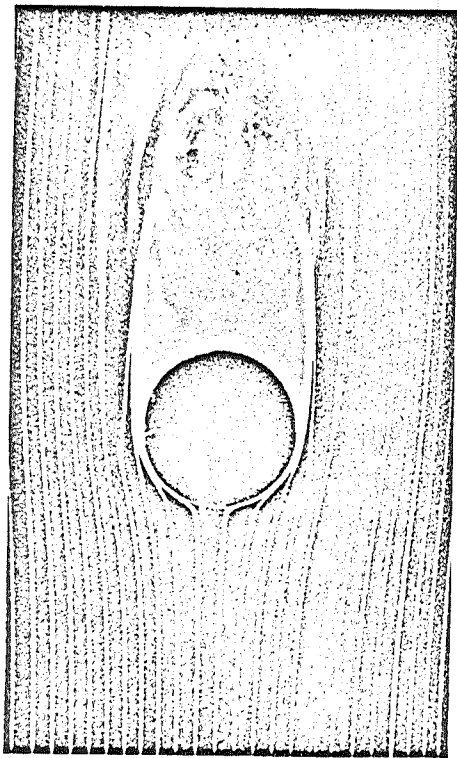


Figure 18. High-velocity flow.

FLOW AROUND A CYLINDER

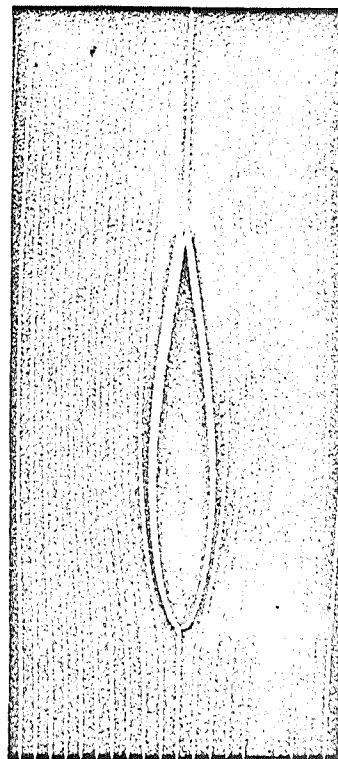


Figure 19. Flow at the center of the section.

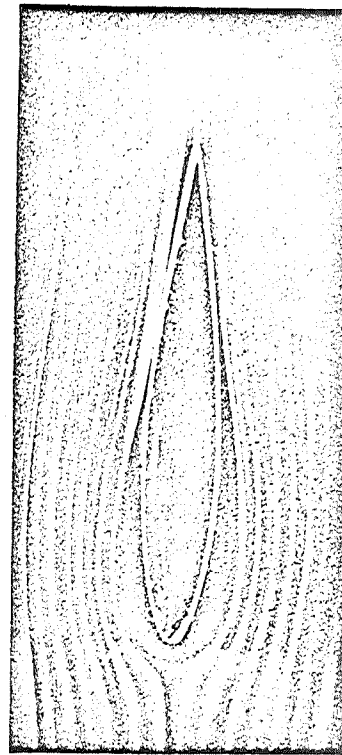
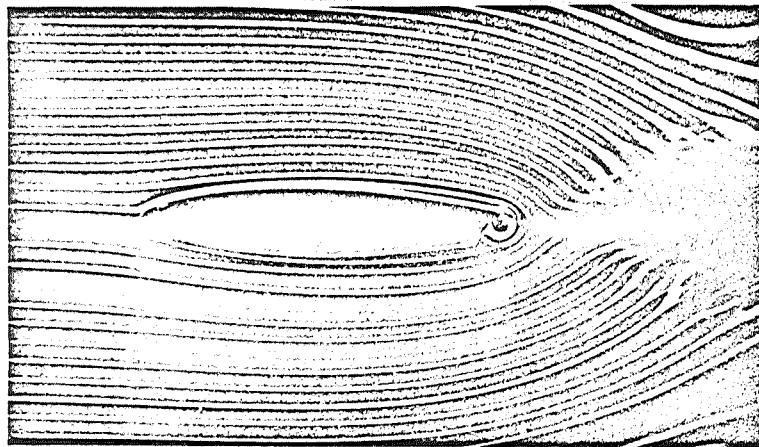


Figure 20. Flow at the wall of the section.

FLOW AROUND A PROFILE AT ZERO INCIDENCE



FLOW AROUND A PROFILE  
WITH ORIENTABLE TRAILING-  
EDGE JET. (Incidence of  
the profile  $i = 0^\circ$ ). /22

Figure 21. Flow with jet directed to the rear  
( $\alpha = 0^\circ$ ).

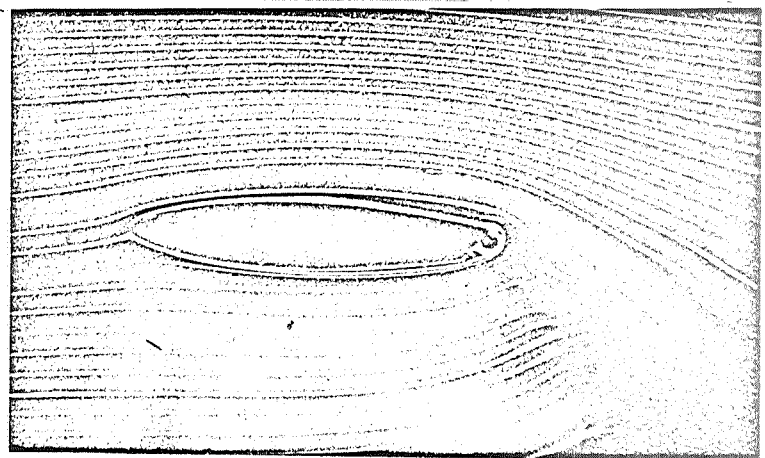


Figure 22. Flow with jet  
directed downwards ( $\alpha =$   
 $= 45^\circ$ ).

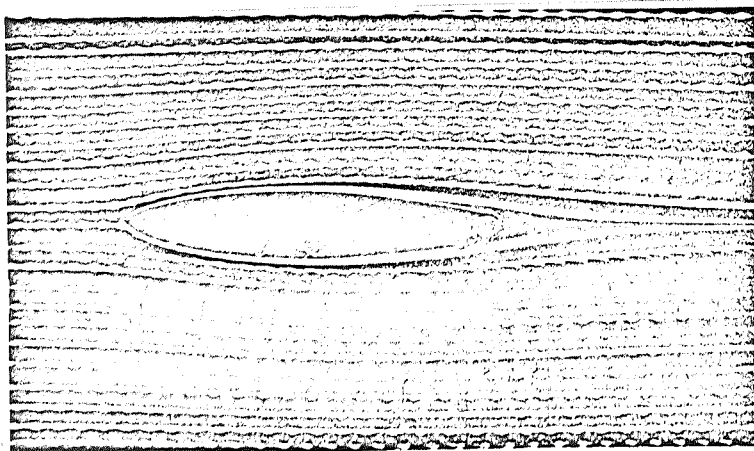


Figure 23. Flow without  
jet (with modulated  
milky injections).

Example No. 4 - "STUDY OF PARIETAL FLOWS"

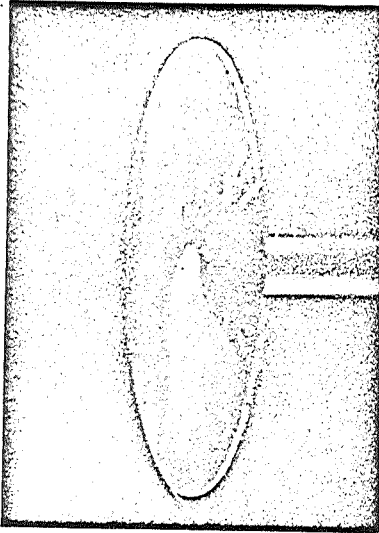


Figure 24. Disk in trans-  
lation normal to its plane.  
Umbilicus is shown.



Figure 25. Parietal flow on the lower  
surface of a flattened ellipsoid.  
Incidence  $i = 2.5^\circ$ . Asymmetrical  
separation. Point of convergence is  
shown (partial view).

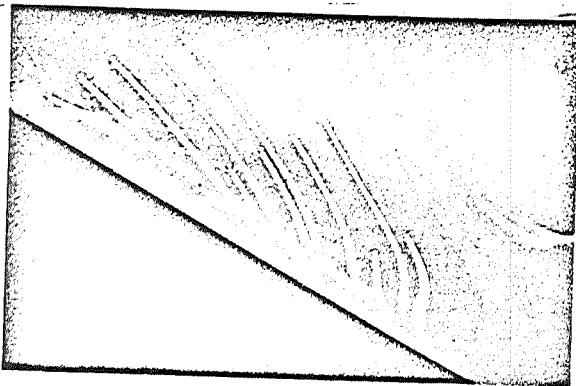


Figure 26. Parietal flow on the  
upper surface of a swept wing.  
Incidence  $i = 14^\circ$ . Thickness  
15%. Line of separation is shown  
(partial view).

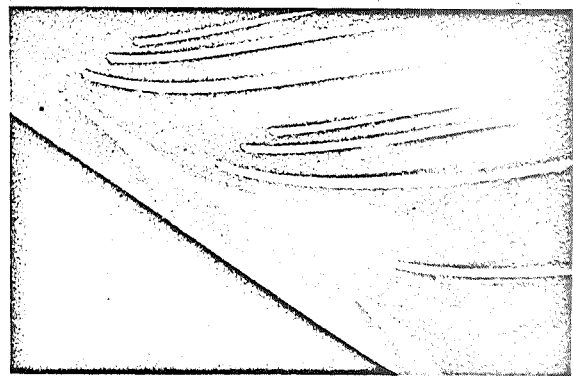


Figure 27. Parietal flow on the  
lower surface of a swept wing.  
Incidence  $i = 17^\circ$ . Thickness  
15%. Line of separation of the  
lower flows (or better, the  
parting line) is shown (partial  
view).

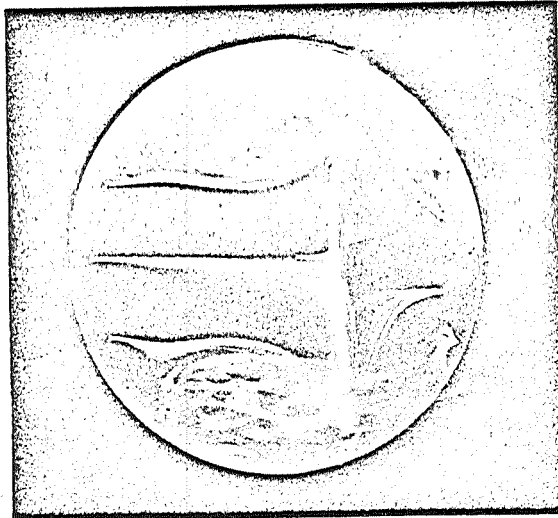


Figure 28. Parietal flow on the upper surface of a flattened ellipsoid of revolution. Incidence  $i = 15^\circ$ . Partition point is shown.



Figure 29. Parietal flow on the lower surface of a rectangular wing of limited span with marginal venting. Zero incidence. Effects of aspirating the fluid flap are shown.

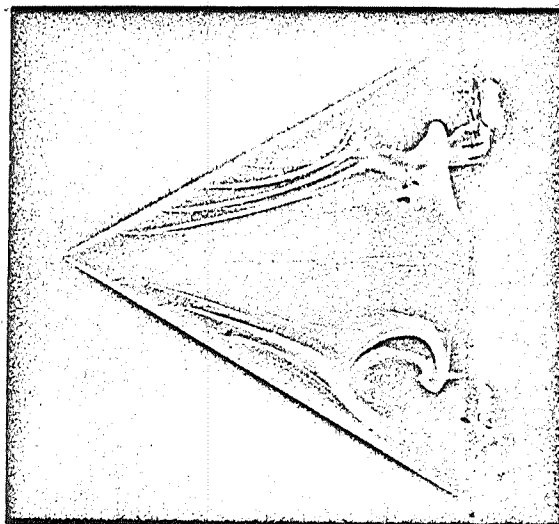
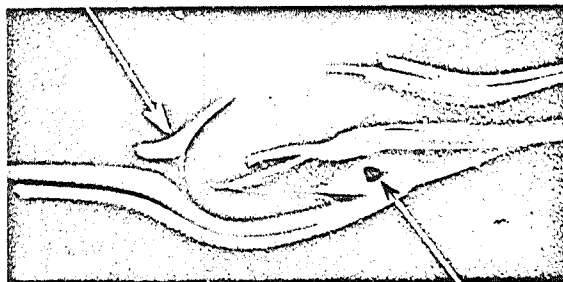


Figure 30. Parietal flow on the upper surface of a thick delta wing (10%). Incidence  $i = 8^\circ$ . Point of spiral convergence is shown.

(1) Partition point



Point of spiral convergence (2)

Figure 31. Mechanism of flow around a vortex generator on the lower surface of a straight wing mounted between the walls (partial view).

Example No. 5 - "STUDY OF VORTICES"

FLOW AROUND A BARE FUSELAGE  
(Incidence  $i = 20^\circ$ ) (Figs. 32, 33, 34)

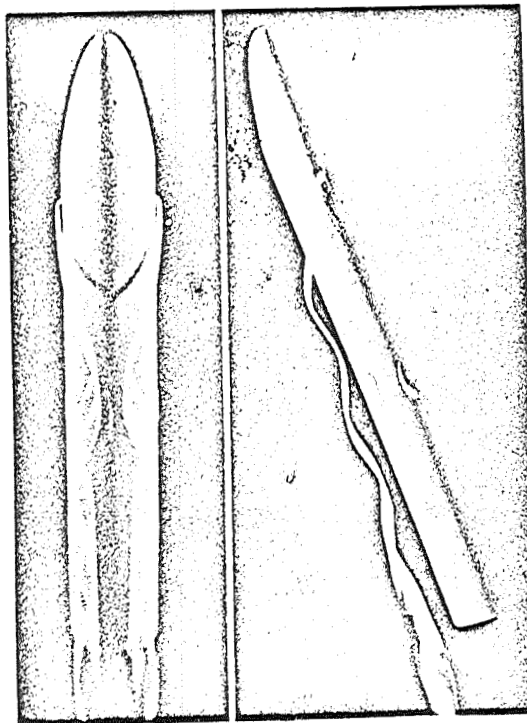


Figure 32. Views of upper surface and profile.

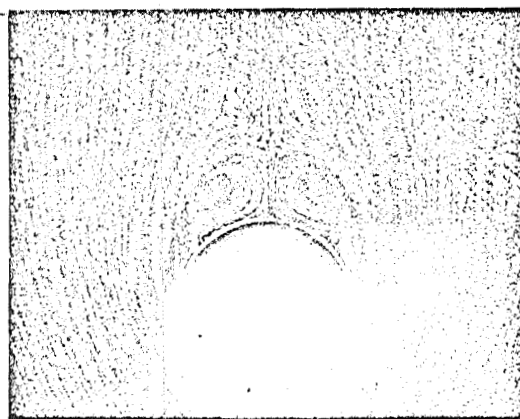


Figure 33. Transverse section of flow at midlength of model (air-bubble method).

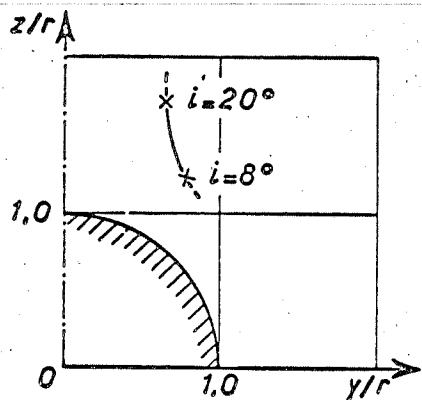
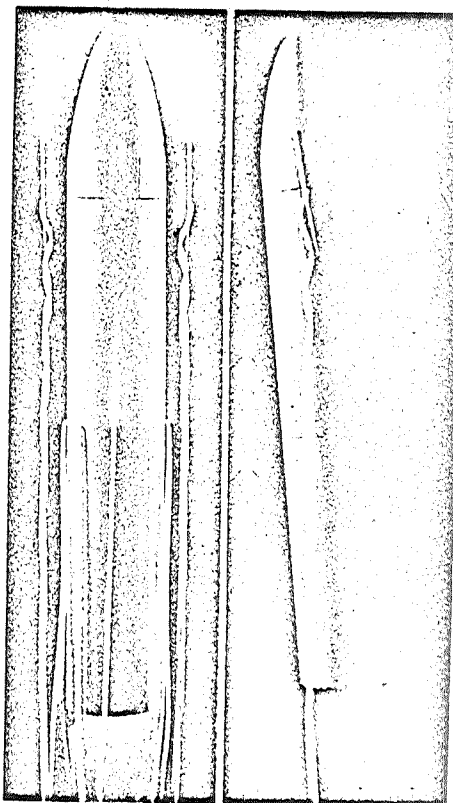
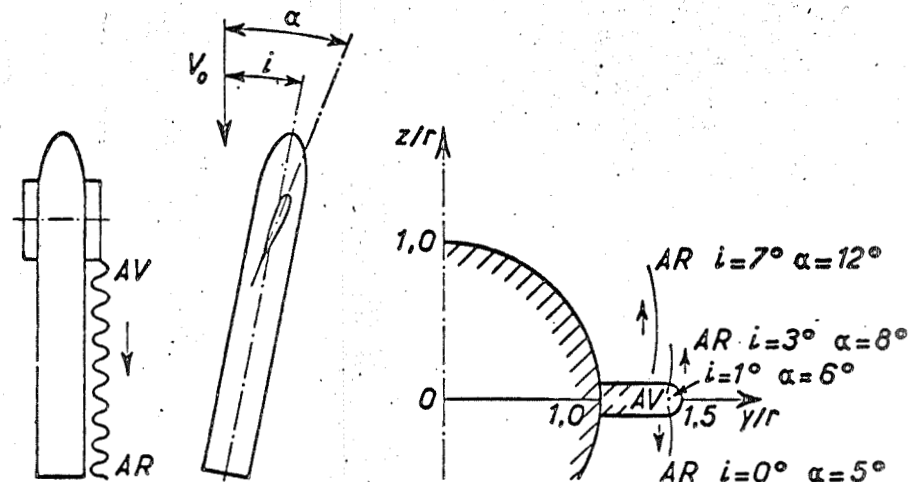


Figure 34. Displacement of the trace of the upper vortex axis in the transverse plane at the end of the fuselage, as a function of incidence  $i$  ( $r$  = radius of fuselage).

Figure 35. Views of upper surface and profile. Incidence of fuselage  $i = 5^\circ$ . Incidence of forward wing  $\alpha = 10^\circ$ .



FLOW AROUND AN IN CANARD MODEL (Figs. 35 and 36)



/26

Figure 36. Influence of incidence on the trajectory of the marginal vortex of the forward wing in the transverse plane (OX corresponds to the longitudinal axis of the fuselage;  $r$  = radius of fuselage).

#### Example No. 6 - "INTERACTION BETWEEN EXTERNAL AND INTERNAL FLOWS"

FLOW AROUND AN ELONGATED ELLIPSOID OF REVOLUTION AT ZERO INCIDENCE IN A STREAM OF VELOCITY  $V_0$  (Figs. 37, 38, 39, 40, 41).

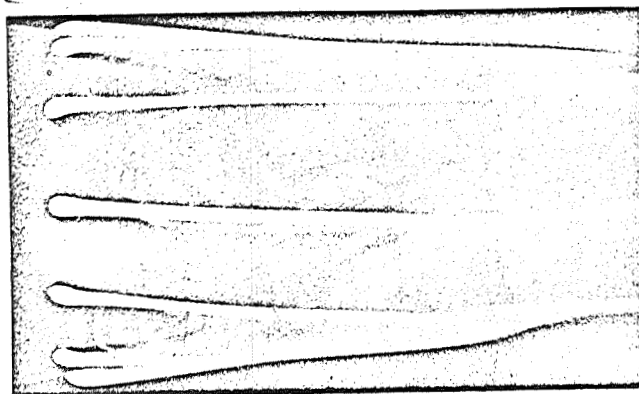


Figure 37. Flow without jet. Colored injections upstream of separation.

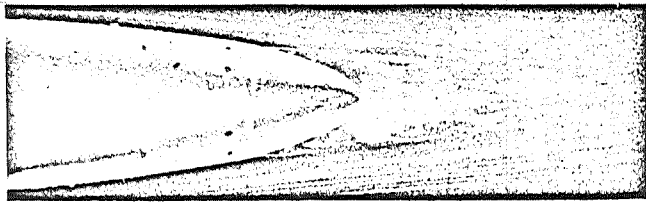
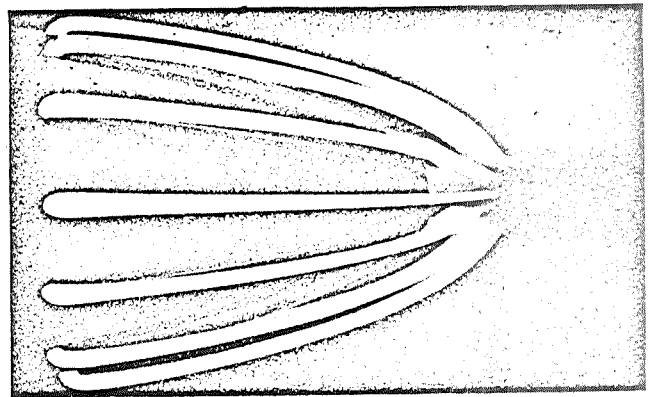


Figure 38. Flow without jet visualized by air bubbles (wake colored by milky injection of short duration into the separated region).

Note - The photos obtained by the air-bubble method represent longitudinal sections of the flow, passing through the axis of revolution of the model.

Figure 39. External flow in the presence of a jet. (Average velocity of jet =  $10 V_0$ ).



/27

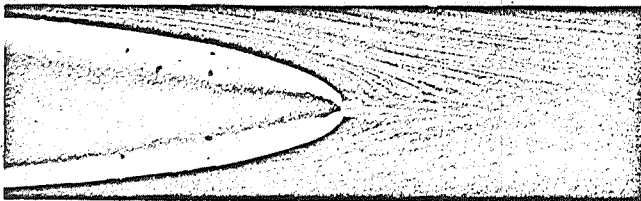
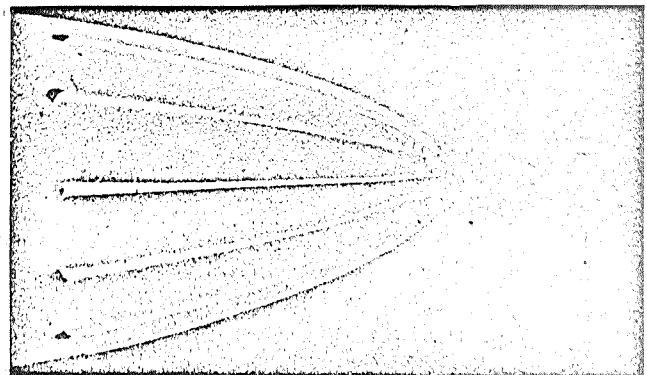


Figure 40. Flow in the presence of a jet visualized with air bubbles. (Average velocity of jet =  $10 V_0$ ).

Figure 41. Parietal flow in the presence of a jet. (Average velocity of jet =  $10 V_0$ ).



Example No. 7 - "STUDY OF SEPARATION NEAR THE LEADING EDGE"

LONGITUDINAL SECTIONS OF THE FLOW (air-bubble method)

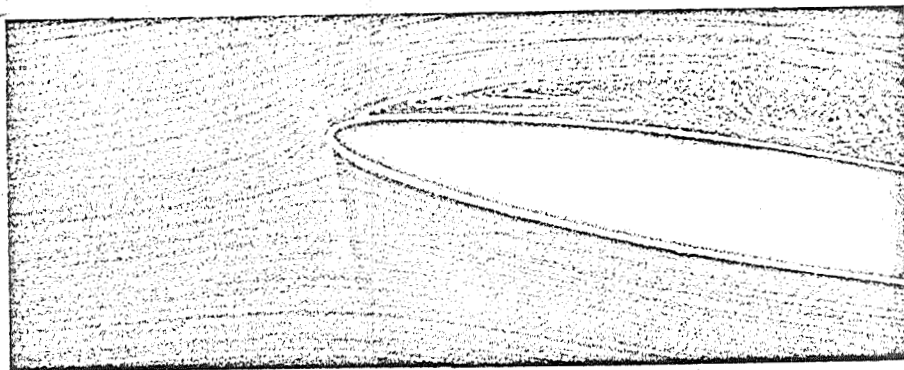


Figure 42. Flow without leading-edge separation (profile NACA 64 A 0 10, zero incidence).

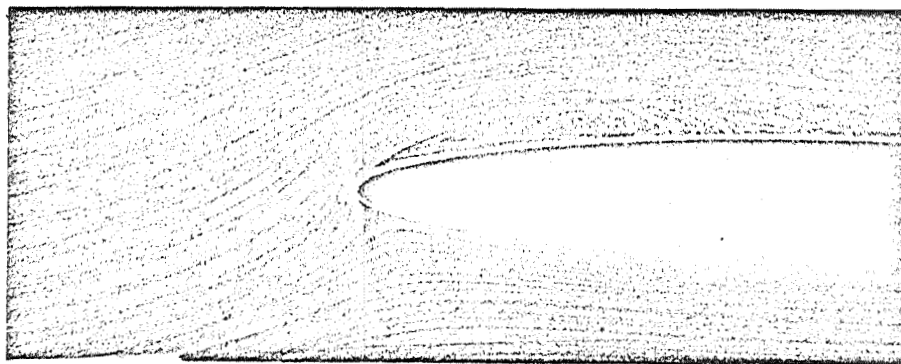
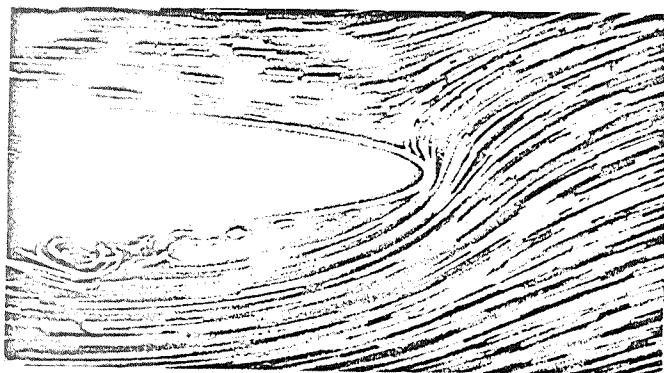


Figure 43. Flow with general separation (profile NACA 64 A 0 10, 10° incidence, no venting).



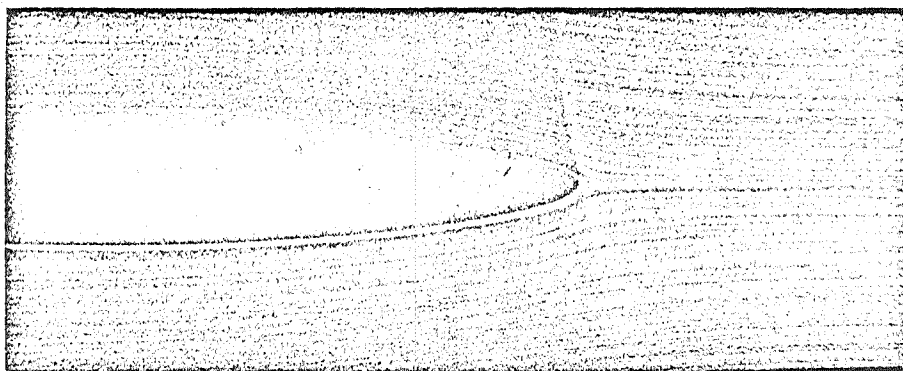
Figure 46.

Figure 45.



Figures 44-45-46.  
Flow with separation bulb  
(profile NACA 64 A 0 10,  
zero incidence, with trailing-  
edge venting): momentum-flow  
coefficient  $C_p = 0.8$ .

Figure 44.



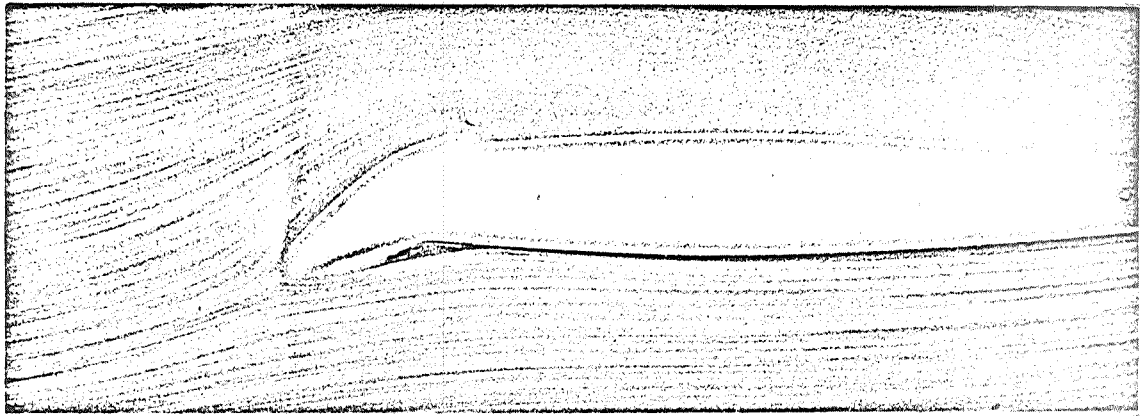


Figure 47. Flow with multiple venting - one tangential jet near the leading edge ( $C_{u_{LE}} = 0.4$ ). - one jet normal to the trailing edge ( $C_{u_{TE}} = 0.8$ ) (profile NACA 64 A 0 10, zero incidence, leading edge broken).

Example No. 8 - "HYPERLIFTING BY A DEFLECTED ENGINE JET"

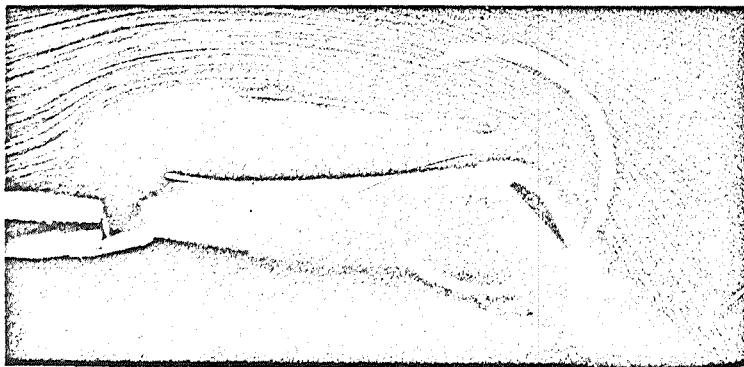
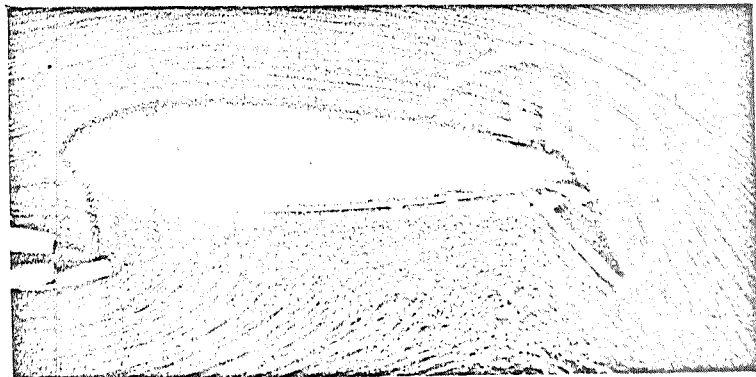
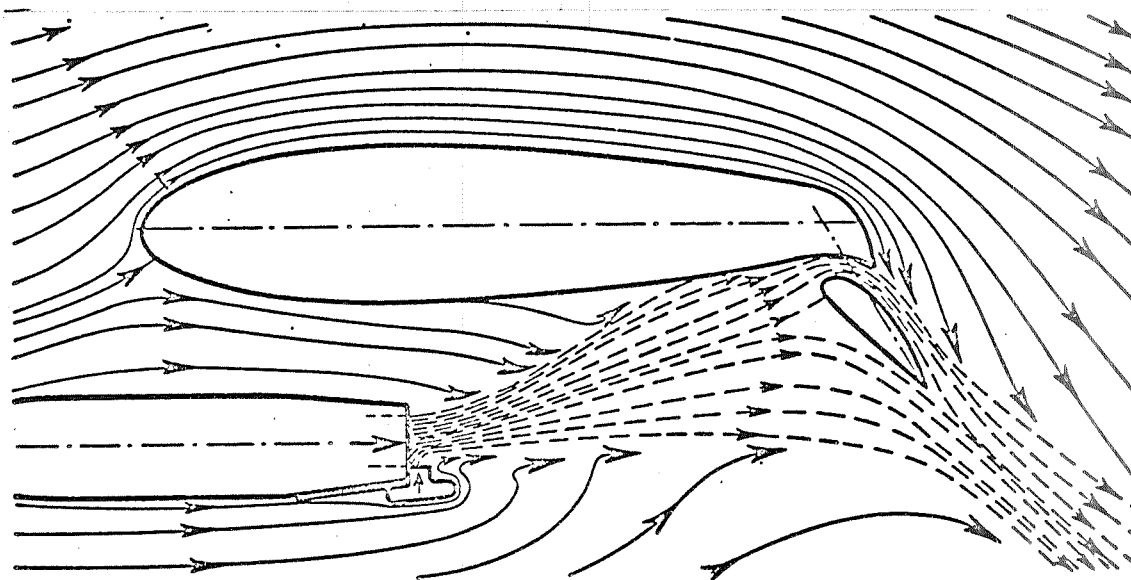


Figure 48. View of flow with mechanical deflection (by flap) of engine jet (in white). Incidence of profile =  $0^\circ$ ; setting of trailing-edge flap =  $55^\circ$ ; average velocity of engine jet =  $12 V_0$ ; advanced engine position.

Figure 49. View of flow with mechanical deflection (by flap) of engine jet (uncolored): Incidence of profile =  $0^\circ$ ; setting of trailing-edge flap =  $55^\circ$ ; average velocity of engine jet =  $15 V_0$ ; advanced engine position.





/30

Figure 50. Diagram of the mechanism of flow for an engine jet deflected by an auxiliary jet.

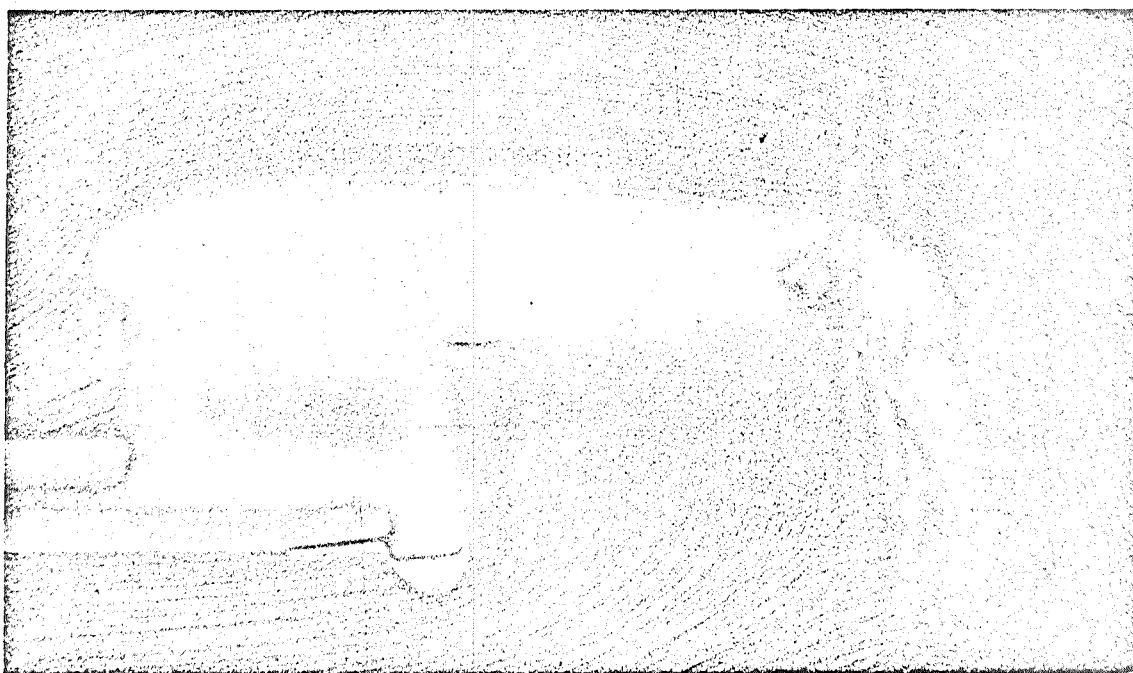


Figure 51. View of flow with pneumatic deflection of the engine jet. Incidence of profile =  $0^\circ$ ; setting of trailing-edge flap =  $75^\circ$ ; average velocity of engine jet =  $15 V_0$ ; retracted position of engine.

$V_0$  = velocity of upstream current

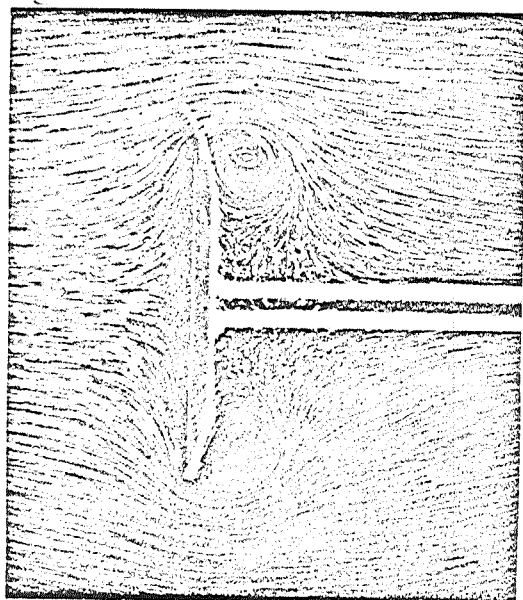


Figure 52. First stage of starting.

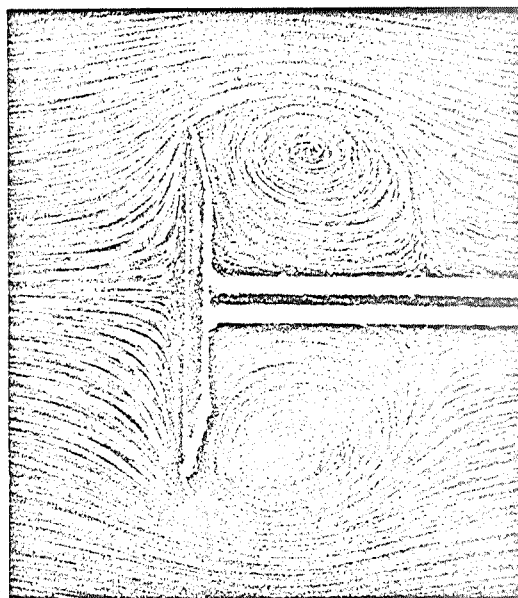


Figure 53. Starting.

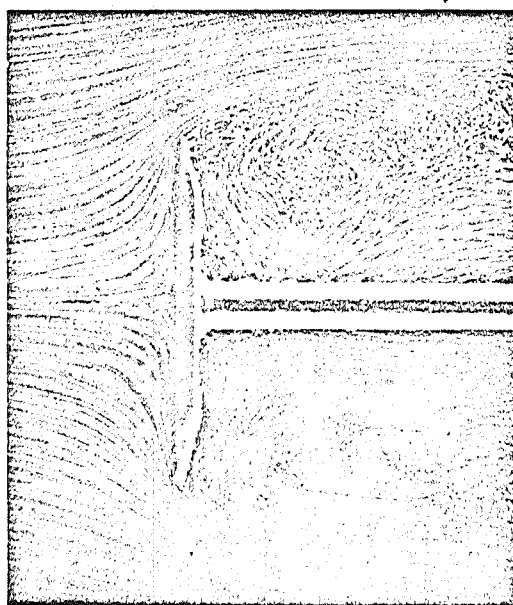


Figure 54. Steady state.

DISK IN TRANSLATION NORMAL TO ITS PLANE (views of the diametral plane).

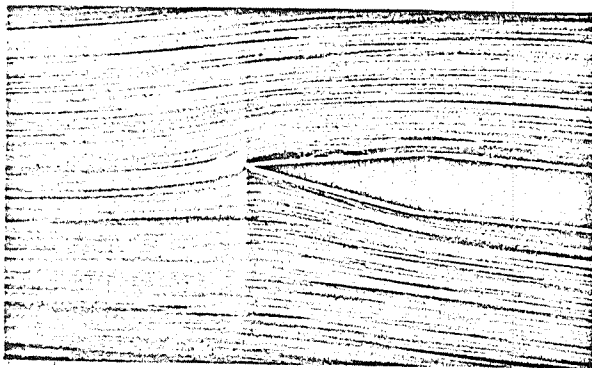


Figure 55. Starting.

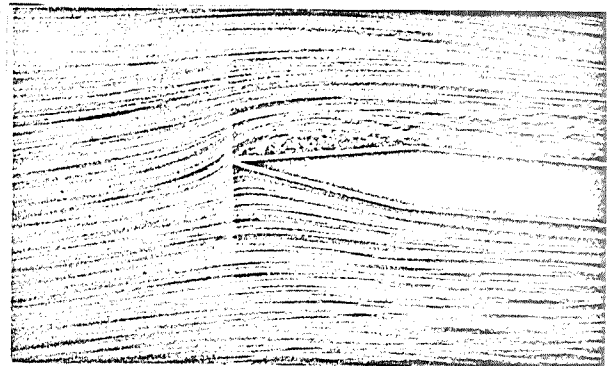


Figure 56. Steady state.

/32

FLOW AROUND A PROFILE WITH SHARP LEADING EDGE, NONZERO INCIDENCE.

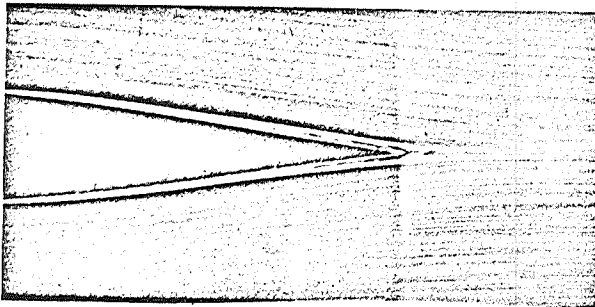


Figure 57. First stage of starting.

Figure 58. Last stage of starting.

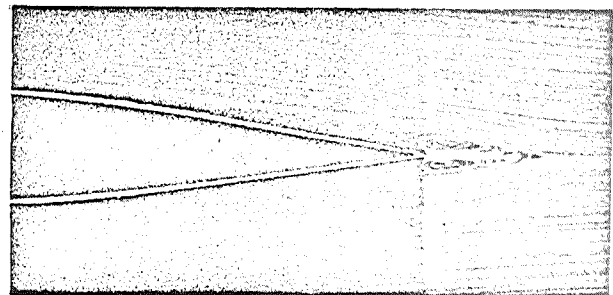
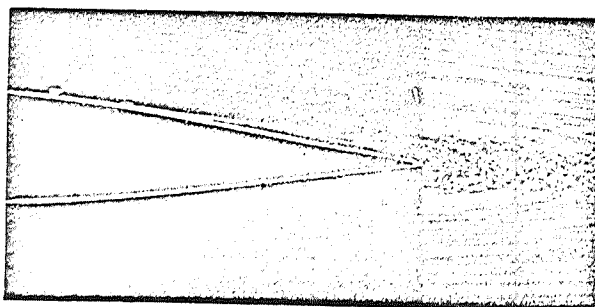


Figure 59. Steady state.



FLOW NEAR THE TRAILING EDGE OF A THICK PROFILE, ZERO INCIDENCE.

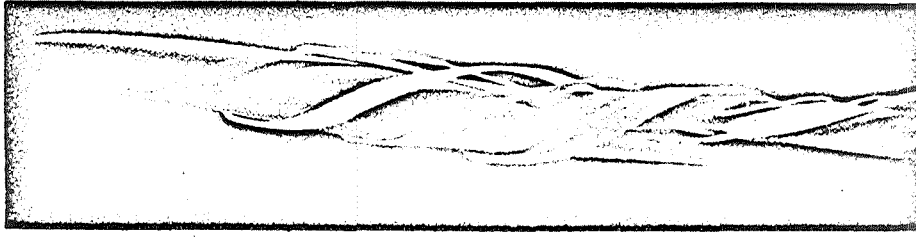


Figure 60. Marginal vortex of a rectangular wing, profile view (incidence  $i = 8^\circ$ ).



Figure 61. Two-dimensional laminar separation (Profile NACA 64 A 0 10, zero incidence).

Modulated injections in the boundary layer ahead of separation (in white) and within the separated region (in rose).

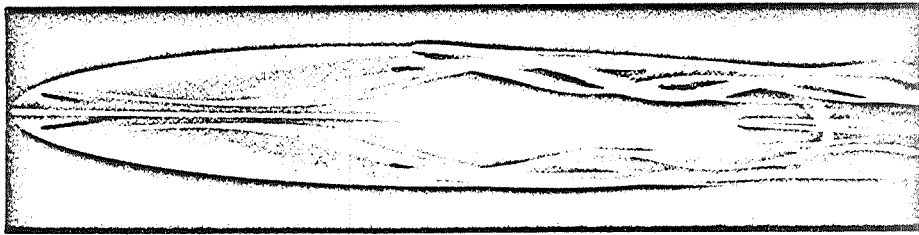


Figure 62. Flow on the upper surface of an elongated ellipsoid of revolution at  $17^\circ$  incidence.

Parietal injections in rose, vortices of the upper surface in white and yellow.

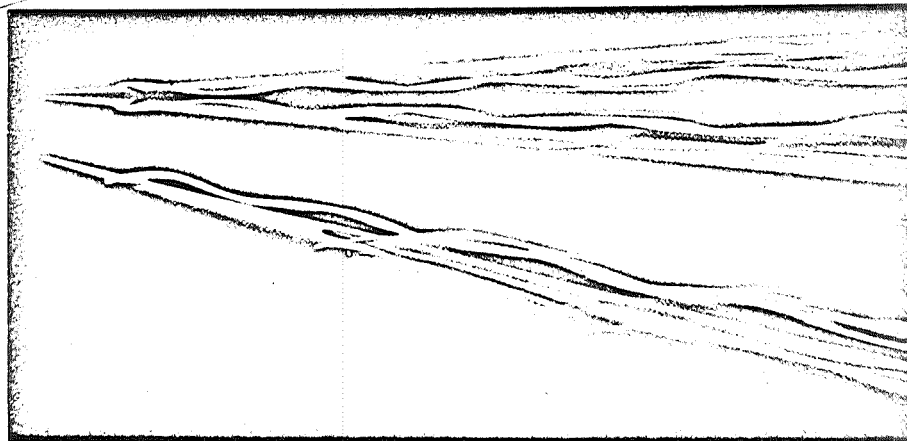


Figure 63. Flow around a conical model.  
Views of upper surface and of profile. Incidence  $i = 20^\circ$ .

FLOW AROUND A THIN DELTA WING WITH POINTED LEADING EDGE

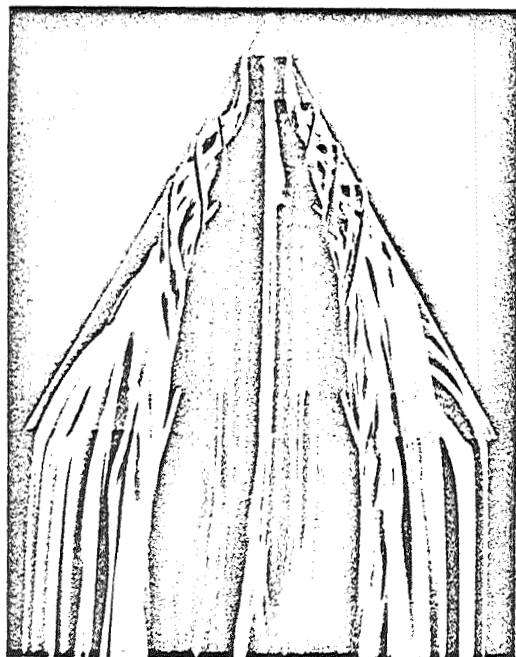


Figure 64. External flow.

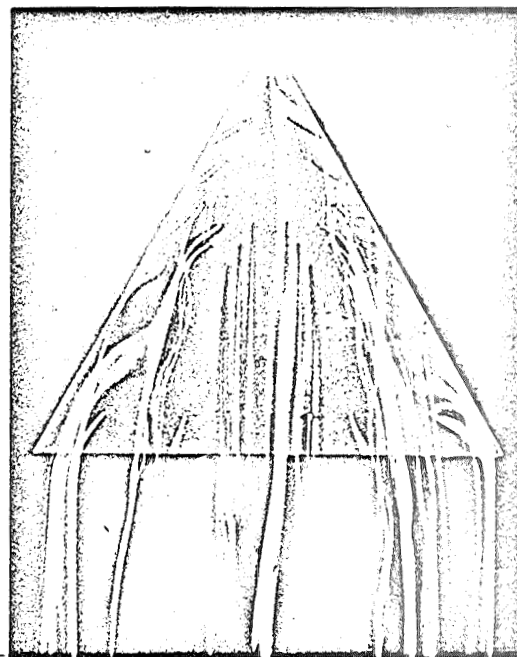


Figure 65. Parietal flow.

Views of the upper surface - Incidence  $i = 3^\circ$

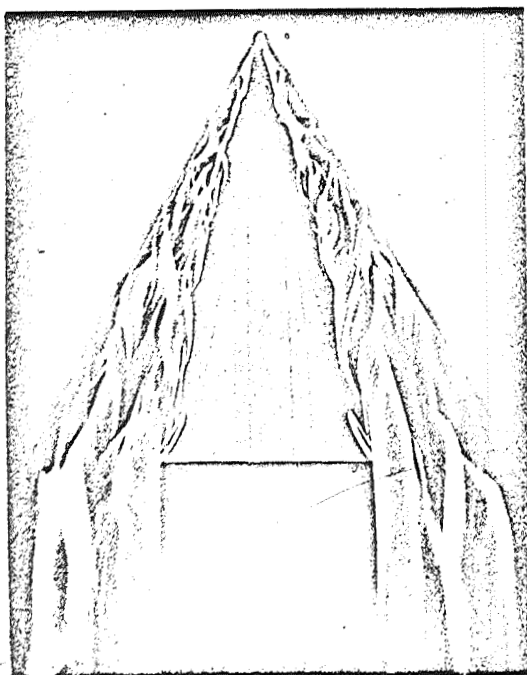


Figure 66. View of the upper surface.

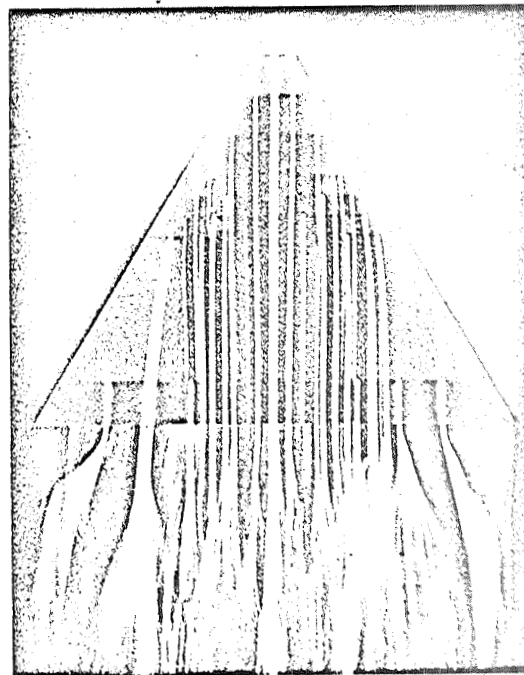


Figure 67. View of the lower surface.

Incidence  $i = 12^\circ$

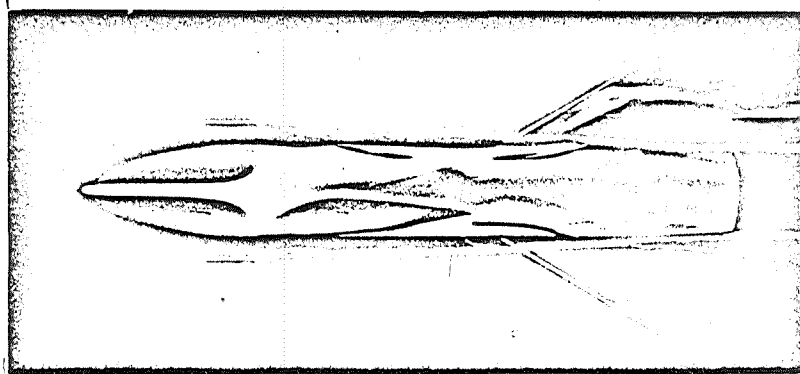


Figure 68. Flow on the upper surface of a model in canard configuration.

Incidence (fuselage, forward wing, after wing):  
 $i = 12^\circ$ . Parietal flow on the fuselage in white and green; cone vortices of the after wing in white and red; marginal vortices of the forward wing in red. The red shade of these latter vortices on the fuselage is due to the lateral lighting, and allows them to be located in space.

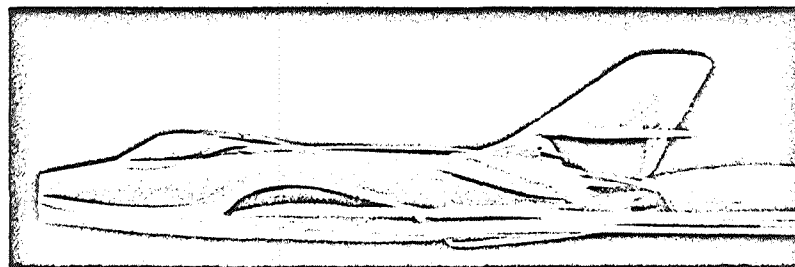


Figure 69. Flow around aircraft model with simulation of engine operation.

Incidence  $i = 0^\circ$ ; average inlet velocity =  $V_0$ ;  
 average velocity of engine jet =  $2 V_0$ . ( $V_0$  =  
 = velocity of upstream current).

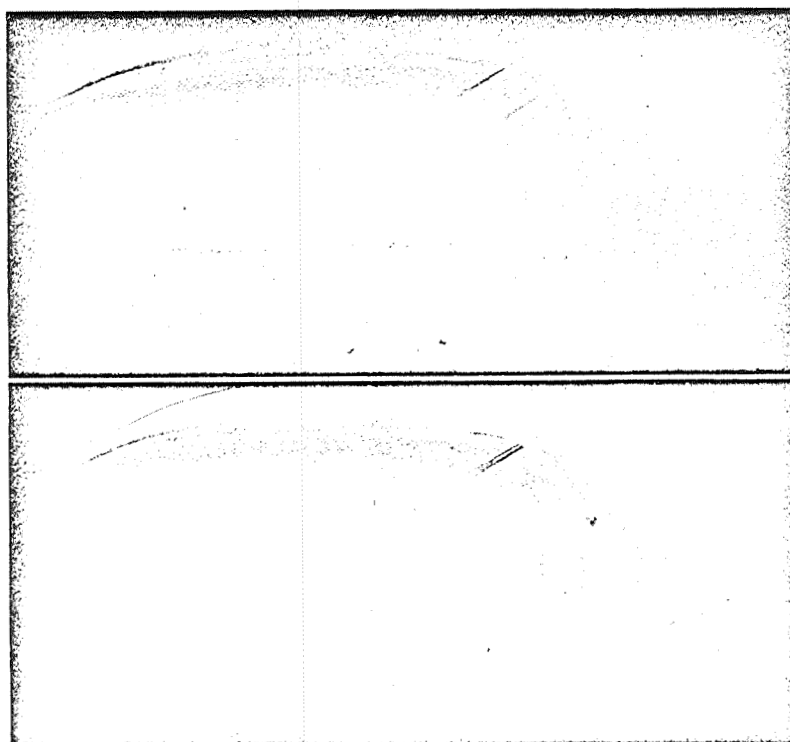


Figure 70. Re-attachment of flow around a wing with vented trailing-edge flap. Incidence of wing  $i = 5^\circ$ ; setting of flap  $\alpha = 60^\circ$ . Above: insufficient venting; below: correct venting.

TRAILING-EDGE VENTING OF A RECTANGULAR WING OF  
LIMITED SPAN, ZERO INCIDENCE (Figs. 71 and 72)

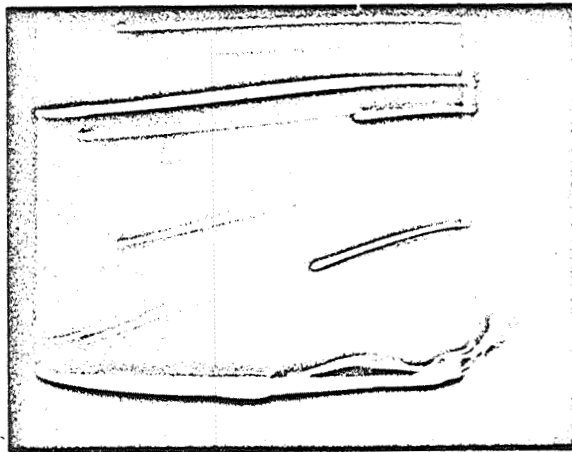


Figure 71. View of upper surface: One can see the marginal vortex due to venting, and outlining of the trailing edge by colored streamlets.

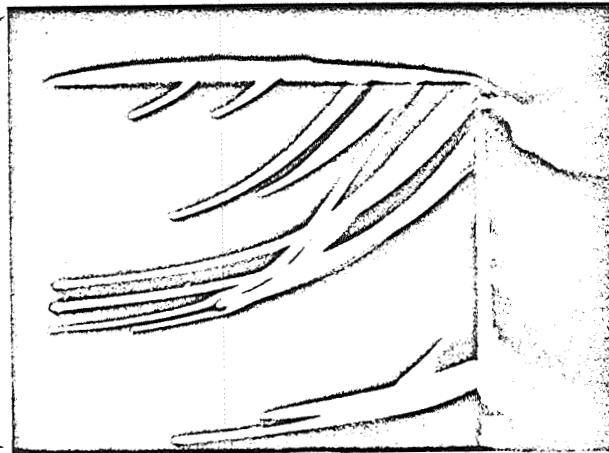


Figure 72. View of lower surface: Part of the colored streamlets is aspirated by the fluid flap issuing from the slit; the rest goes on to feed the marginal vortex.

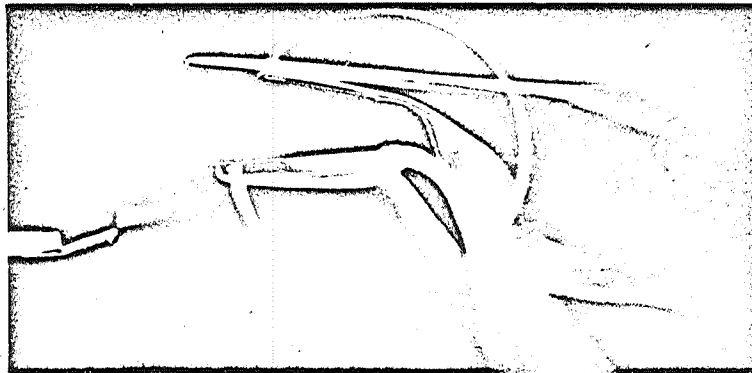


Figure 73. Wing with trailing-edge flap and jet engine mounted in a pod, with jet deviated by flap. Incidence of wing  $i = 0^\circ$ ; setting of flap  $\alpha = 55^\circ$ . (Flow without jet in blue; flow in jet in rose and yellow).

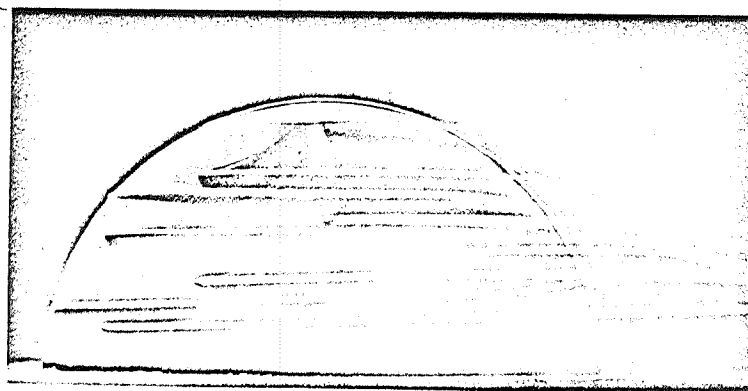


Figure 74. Peripheral venting of a flattened ellipsoid of revolution, zero incidence (view of lower surface). (Flow without venting in green; flow with venting in red).